

NOAA Technical Memorandum NWS HYDRO-23

STORM TIDE FREQUENCY ANALYSIS FOR THE
COAST OF PUERTO RICO

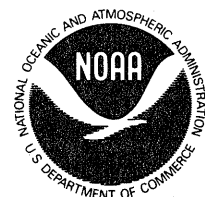
Francis P. Ho

Office of Hydrology
Silver Spring, Md.
May 1975

UNITED STATES
DEPARTMENT OF COMMERCE
Rogers C. B. Morton, Secretary

NATIONAL OCEANIC AND
ATMOSPHERIC ADMINISTRATION
Robert M. White, Administrator

National Weather
Service
George P. Cressman, Director



STORM TIDE FREQUENCY ANALYSIS
FOR THE COAST OF PUERTO RICO

CONTENTS

	Page
Abstract	1
1 Introduction	1
1.1 Objective and scope of report	1
1.2 Authorization	2
2 Summary of historical hurricanes	3
2.1 Introduction	3
2.2 Hurricane tracks	3
2.3 Historical notes	3
2.3.1 September 12-19, 1876	3
2.3.2 August 18-25, 1891	3
2.3.3 August 13-25, 1893	3
2.3.4 August 3-24, 1899	4
2.3.5 August 21-25, 1916	4
2.3.6 September 6-20, 1928	4
2.3.7 September 8-16, 1931	4
2.3.8 September 25-October 3, 1932	5
2.3.9 August 9-19, 1956 - BETSY	5
3 Climatology of hurricane characteristics	7
3.1 Hurricane parameters and frequency	7
3.2 Definition	7
3.3 Data sources	7
3.4 Probability distribution of hurricane central pressure	8
3.5 Probability distribution of radius of maximum winds	9
3.6 Probability distribution of speed of storm motion	9
3.7 Frequency of tropical cyclone tracks	10
3.7.1 Seaward alongshore storms, San Juan	10
3.7.2 Landward alongshore storms, San Juan	10
3.7.3 Landward alongshore storms, south coast	10
3.7.4 Seaward alongshore storms, south coast	10
3.7.5 Landfalling storms, south coast	10
3.7.6 Exiting storms, north coast	10
3.7.7 West coast	11
3.7.8 East coast	11
3.8 Track density method	11
3.8.1 Track frequency	11
3.8.2 Direction probability	12
3.8.3 Application at a point	12
3.8.4 Landfalling frequency on southern coast	12
3.9 Probability distribution of tropical cyclone direction of motion	12

	Page
4 The hurricane surge model	15
4.1 The model	15
4.2 Application of model to Puerto Rico	15
5 Storm tide frequencies by joint probability method	17
5.1 Example--San Juan	17
5.2 West coast	18
5.3 South coast	18
5.4 Extrapolation to uncharted areas	18
5.5 Pressure-wind relationship	19
6 Wave effects	23
6.1 Introduction	23
6.2 Wave problem in Puerto Rico	23
6.3 Wave swash study for extratropical storms	23
6.4 Estimated hurricane effects	24
7 Demarcation of flood prone limits	25
7.1 Objective	25
7.2 Precipitous coastal areas	25
7.3 Flat coastal areas	25
References	26
Figures	27-43

NOTE

This report was prepared for the Federal Insurance Administration by the National Weather Service, NOAA, in August 1973. It is being issued in this form for wider distribution.

STORM TIDE FREQUENCY ANALYSIS FOR THE COAST OF PUERTO RICO

Francis P. Ho
Special Studies Branch, Office of Hydrology
National Weather Service
Silver Spring, Md. 20910

A report on work for the Federal Insurance Administration
Department of Housing and Urban Development by National
Oceanic and Atmospheric Administration, Department of Commerce

ABSTRACT

Storm tide height frequency distributions on the coast of Puerto Rico are developed for the National Flood Insurance Program by computing storm tides from a full set of climatologically representative hurricanes, using the National Weather Service hydrodynamic storm surge model adapted to local conditions. Hurricane parameters needed for the storm tide computation are analyzed and presented.

Tide levels for the southern coast of Puerto Rico are shown in coastal profile between annual frequencies of 0.10 and .002. Similar tide levels for San Juan on the northern coast and Mayaguez on the western coast are also presented, and tentative interpolated tide levels of .01 annual frequency for the remaining coasts. Wave effects on the north coast are discussed.

Chapter 1

INTRODUCTION

1.1 Objective and scope of report

The Federal Insurance Administration (FIA), Department of Urban Development (HUD), requested the National Oceanic and Atmospheric Administration (NOAA) to delineate the 100-year flood line from storm tides on the coast of Puerto Rico. This study is part of the survey of the whole United States by FIA to delineate those areas and communities subject to flooding, required by Section 1360(1) of the National Flood Insurance Act of 1968 and is called a "Type 7" study by the FIA. Over much of the

United States this type of delineation, more limited than a flood insurance rate-making study ("Type 15"), has proceeded quadrangle by quadrangle of the U. S. Geological Survey topographic series, from readily available stream flow or tidal data.

For coastal Puerto Rico there are no such readily available storm tide data. Therefore, NOAA found it necessary to develop data in the same series of steps used in hurricane zones on the mainland coast for "Type 15" rate-making flood frequency analyses. These steps are: (a) establish the climatological frequency of certain hurricane parameters from past storms, (b) construct smoothed-out depictions of the sea surface bottom from the coast to a 300-foot water depth, (c) compute storm surges for various coastal points from representative climatological hurricanes with a hydrodynamic model, (d) add the storm surge to astronomical tide at various phases, (e) collect the computed total storm tide elevations into a flood frequency diagram, (f) read 100-year flood levels from these diagrams, and (g) construct the 100-year flood line on maps, making allowances for wave action on the immediate beach front. A locator map and smoothed off-shore water depths are shown in Figure 1-1.

In view of the reconnaissance intent of the study, short cuts were taken wherever possible. However, the basis has been laid for a rate-making "Type 15" study if this should be undertaken in the future.

1.2 Authorization

The National Flood Insurance Act of 1968, Title XIII, Public Law 90-448, enacted August 1, 1968, authorizes and directs the Secretary of Housing and Urban Development to establish and carry out a National Flood Insurance Program. The Secretary is authorized to secure the assistance of other Federal Departments or other agencies on a reimbursement basis in identifying flood-plain areas, including coastal areas. Authorization for this particular study is Project Order No. 4, Agreement No. IAA-H-5-73 dated May 2, 1973, between the Federal Insurance Administration (FIA) of the Department of Housing and Urban Development (HUD) and NOAA.

Acknowledgment

Three components of NOAA collaborated on the Puerto Rico assignment. The hurricane climatological analysis and computation of tide levels are by the Special Studies Branch, Office of Hydrology, National Weather Service. Definition of the Bathymetry (water depth) and adaptation of the storm surge computation model to Puerto Rico are by the Storm Surge Unit, Techniques Development Laboratory of the Systems Development Office, National Weather Service. Map preparation and coordination are by the Coastal Mapping Division, National Ocean Survey.

The study was funded by the Federal Insurance Administration, Department of Housing and Urban Development.

CHAPTER 2

SUMMARY OF HISTORICAL HURRICANES

2.1 Introduction

This chapter summarizes the hurricanes that have moved across the island of Puerto Rico since 1871. A few of the lesser storms are omitted. Prior to the year 1871, there were three prominently noted hurricanes which inflicted severe damage to the island. These are the hurricanes of Santa Ana on July 26, 1825; Los Angeles on August 2, 1837; and San Narciso on October 29, 1867. It is customary in Puerto Rico to name a hurricane after the saint on whose day it happens to occur. There were no meteorological data available on these storms and records are incomplete and inaccessible.

2.2 Hurricane tracks

The tracks of the hurricanes are shown in Figure 2-1.

2.3 Historical notes

Brief notes on the history and damages caused by the hurricanes abstracted from published papers follow:

2.3.1 September 12-19, 1876

The center of this storm entered Puerto Rico between Humacao and Yabuca and exited between Rincon and Mayaguez. The lowest barometric pressure recorded was 989.5 mb (29.22 in.) at San Juan. This storm was extremely destructive. In the San Juan area, 45 ships were lost and severe damage was done in the land areas.

2.3.2 August 18-25, 1891

One of the most disastrous of West Indian hurricanes occurred on August 18-19, 1891. Its center approached Puerto Rico from the southeast, passing through Martinique on August 18th and causing \$10 million damage and the loss of 700 lives on that island. The storm entered Puerto Rico on August 19th and exited the north coast later that evening. The storm was of small diameter but of great intensity. This storm was referred to as the Martinique hurricane

2.3.3 August 13-25, 1893

This tropical storm was first detected on August 13 southeast of the Windward Islands moving in a northeasterly direction. Its center

entered the southeast coast of Puerto Rico near Punta Guayama in the afternoon of the 16th and exited the island near Isabela. The lowest barometric pressure recorded at San Juan was 988 mb (29.17 in.).

2.3.4 August 3-24, 1899

One of the most destructive hurricanes in Puerto Rican history passed directly across the entire length of the island on August 8. The storm has become known as "San Ciriaco." More than 3,000 lives were lost, mostly from drowning. Property loss was enormous. The storm center entered near Arroyo on the southeast coast at about 8 a.m. and the calm in the "eye," or center, lasted about 15 minutes. The barometric pressure fell to 939.7 mb (27.75 in.). The maximum wind speed at Arroyo was estimated at about 90 knots. A storm tide destroyed almost all of the houses at the port of Humacao on the east coast. Destructive winds and torrential rains accompanied the hurricane in its progress across the island. Between 1 and 2 p.m. the center left the island near Aguadilla on the west coast.

2.3.5 August 21-25, 1916

This small size storm moved across Puerto Rico in an east to west direction on August 22. Its center passed just south of San Juan which experienced a maximum wind of about 80 knots, and a minimum barometric pressure of 997 mb (29.44 in.). An estimated million dollars damage was inflicted in Puerto Rico by this storm along its path of about 45 to 50 miles in width.

2.3.6 September 6-20, 1928

The most intense hurricane of the 20th century to strike Puerto Rico was first reported at about 300 miles east of the Leeward Islands. Its center moved west-northwestward and entered the southeast coast of Puerto Rico, near Guayama. The hurricane moved across the island at an average speed of about 11 knots and exited the north shore between Aguadilla and Isabela. A minimum barometric pressure (931.3 mb or 27.50 in.) in the vicinity of Puerto Rico was reported by the steamship Matura located at about 10 miles south of the island of St. Croix. The lowest barometric pressure recorded at Guayama was 936.3 mb (27.65 in.) Maximum winds of about 130 knots were recorded at San Juan, some 30 miles to the north of the hurricane center. Winds of hurricane force were experienced throughout the island to the north of the path. Approximately 300 persons in Puerto Rico lost their lives in this storm. Hundreds of thousands of people lost their homes during the storm passage. Property and crop losses were estimated at about \$50 million.

2.3.7 September 8-16, 1931

This hurricane which was named after San Nicolas raked the north coast of Puerto Rico on September 10. The storm had almost developed

into hurricane intensity when it passed to the north of the Virgin Islands. By the time it reached San Juan, hurricane winds were estimated at about 80 knots and a low barometric pressure of 987.8 mb (29.17 in.) was reported. The hurricane moved in a westward direction along the entire north coast of Puerto Rico. Damage caused by the storm was confined to a strip of 5 or 6 miles in width extending from San Juan to Aguadilla.

2.3.8 September 25-October 3, 1932

This hurricane is known as "San Ciprian" in Puerto Rico. Its center crossed the island on September 26, entering the eastern shore near Ceiba in the evening. A barometric pressure of 938 mb (27.70 in.) was recorded on board of the S. S. Jean in the harbor of Ensenada Honda. A minimum pressure of 980.4 mb (28.95 in.) was recorded at San Juan as the center of the hurricane passed some distance to the south, with estimated maximum winds of more than 100 knots. 225 lives were lost in Puerto Rico and 3,000 or more persons were injured in this storm. An estimated 75,000 to 250,000 persons were left homeless after the storm passage. Property damage in the island was estimated at \$30 million.

2.3.9 August 9-19, 1956 - BETSY

Hurricane BETSY was first detected on August 9 to the east of the Lesser Antilles. Its center moved westward to west-northwestward and passed over the island of Guadeloupe, F.W.I., on August 11. Continuing on its west-northwestward course, the hurricane reached the southeastern coast of Puerto Rico on the 12th. The center of hurricane BETSY entered the coast near Guayama and exited the northern coast of the island near Arecibo at an average speed of 18-19 knots. A minimum sea level pressure of 983 mb (29.03 in.) was recorded at Guayama shortly after the hurricane entered land. A minimum pressure of 987 mb (29.15 in.) was recorded at Ramey AFB at about 14 n. mi. to the south of the center. Based on this observation, Colón [1] estimated a central pressure of 973 mb (28.73 in.) for the hurricane as it exited the northern shore. Maximum winds of 100 knots were reported by reconnaissance aircraft on August 10 when the hurricane was located some distance to the west of Puerto Rico. The maximum wind speed of about 65 knots with gusts to 80 knots was recorded at San Juan airport. Sixteen persons lost their lives in the storm in Puerto Rico and the damage inflicted on the island was estimated at \$40 million.

CHAPTER 3

CLIMATOLOGY OF HURRICANE CHARACTERISTICS

3.1 Hurricane Parameters and Frequency

The hurricane parameters needed for storm tide computation are: central pressure, radius of maximum winds, direction of motion relative to the coast, and the speed of forward motion. If track is parallel to the coast, then distance from the coast is needed instead of direction.

Probability distributions are required for each of these parameters to evaluate tide frequencies. Also needed is the overall frequency with which hurricanes enter the coast in terms of strikes per mile per year, or some equivalent unit, and frequency with which hurricanes pass parallel to the coast within certain discrete distances. Storms exiting the coast are also counted where significant.

3.2 Definition

For convenience, a distinction is made in this chapter between "frequency" and "probability." Frequency is defined as the number₁ of occurrences of some event per year and has dimensions of time while probability is the fractional part of a total and is dimensionless.

3.3 Data sources

The data for probability distributions of the variables central pressure, radius of maximum winds, and forward motion are primarily from Navy reconnaissance flights for the period 1945 through 1972. Only storms reported to reach hurricane intensity (winds > 64 knots) are used in this part of the study. These flight data are abstracted from Annual Tropical Storm Reports of the U. S. Navy [3] and from original flight data obtained from the National Climatic Center. Colón and Dunn and Miller [ref. 1 and 4] furnished additional values.

The statistics on the frequency of storm occurrences and on direction of storm motion in this report are based on the yearly storm track charts by Cry [2] from 1871-1963 and from Monthly Weather Review articles between 1964-1972. Both hurricanes (winds greater than 64 knots) and tropical storms (maximum wind 34 to 64 knots) are included in the statistics since the distinction on the track charts is not always clear. Storms classified as "tropical depressions" (less than 34 knots) are not included.

3.4 Probability distribution of hurricane central pressure

Hurricane surges vary directly with the depression of the storm's central pressure below a representative peripheral pressure, other factors being equal. Thus, central pressure is a convenient intensity index. The real driving force for the surge is the stress of the wind on the water, roughly proportioned to the square of the wind speed. But the wind speed squared results from its driving force, the pressure depression. To obtain a probability distribution of central pressures, reports over the area bounded by latitude 15-20°N and longitude 65-70°W were examined during the period of 1945 through 1972 and are believed complete. A list of hurricanes (wind reported > 64 Kt) and their adopted parameters are shown in Table 3-1. The central pressure of the August 1956 hurricane is from adjusted minimum pressure for Ramey AFB after Colón [1] and the central pressure for hurricane EDITH of September 1963 is from Dunn and Miller [4]. Both of these pressure values are lower than the minimum pressure reported by reconnaissance aircraft over the study area.

Figure 3-1 shows the probability distribution of hurricane central pressure based on the Table 3-1 values. To fit a curve to these data that refers to the same statistical population of storms as the track frequency count to be described later, we proceed in the same manner as in an earlier report ([5] p. 12). The track frequency count includes both "hurricanes" and "tropical storms." The data points were plotted by using the formula $P = (M-0.5)/N$, where

- P = accumulative probability
- M = "rank" of observation
- N = number of observations.

By track chart count there were 29 tropical cyclones ("tropical storms" plus "hurricanes") through the study area during the 28 study years. Only 17 central pressures are listed in Table 3-1. These are assumed to cover the "hurricane" range. N in the formula is then 29 and the pressures are arrayed and plotted as if they were the 17 most intense cases of 29. A curve is then drawn by eye to the data and extended smoothly to cover the "tropical storm" range.

The central pressures reported by aircraft for the less intense hurricanes seem too high to support winds of hurricane intensity. Possibly the reported minimum pressure does not coincide with the actual minimum central pressure due to the uncertainty in determining the exact location of a hurricane center when its eye wall was not well defined (which is often the case in a storm barely reaching hurricane intensity). For these reasons the fitted curve is pulled to the left of the upper eight points plotted in the diagram.

For comparison with an adjacent area for which longer quantitative records are available, Figure 3-2 shows, on the same graph, the probability distribution of tropical cyclone central pressures for the Puerto Rico area (18°N) from Figure 3-1 and the southern tip of Florida (25°N) from [6]. There is a difference of about 10 mb if the percentage of storm occurrences is compared level for level. The Puerto Rico curve is comparable to the Palm Beach-Daytona Beach reach of the Florida east coast in [6]. If this 28-year sample is representative, tropical cyclones originating in the Caribbean Sea may not reach their full intensity in the Puerto Rico area.

3.5 Probability distribution of radius of maximum winds

In all hurricanes, proceeding from the storm center outward, winds increase from low values at the center of the eye to their most intense velocity just beyond the edge of the eye, then decrease. The average distance from the storm center to the circle of maximum wind speed is called the radius of maximum winds (R) and is adopted as a convenient single number to be used as an index of the size or lateral extent of the hurricane, a factor which affects the surge profile along the coast. Most of the R's in Table 3-1 are the average distance from center to the maximum wind belt, from the aircraft reports. Where the distance range for this band was quite wide, additional guidance was obtained from the reported radar eye radius, adjusted to R by using the radar eye radius-R-central pressure diagram from Shea ([7] - figure 26.)

The probability distribution of the radius of maximum winds for hurricanes in the Puerto Rico area is shown in Figure 3-3. The curve reveals that more than 50% of the storms passing the study area were small in size ($R < 12$ n. mi.). This is consistent with small size storms generally observed in tropical latitudes. Only about 20% of the storms had R greater than 15 n. mi. The minimum R in the sample of this study was 4 n. mi.

3.6 Probability distribution of speed of storm motion

The probability of distribution of the speed of forward motion of hurricanes in the vicinity of Puerto Rico from the data in Table 3-1 is shown in Figure 3-4. The height of surge on the coast increases with increasing storm speed within the range of observed values in the study area [9] because of dynamic effects in the water. Thus, the occasional fast-moving storms, especially if they are large, pose the greatest hazard.

Only one hurricane had a speed of 22 knots. The absence of high speed of forward motion is characteristic of low latitudes. An inspection of hurricane tracks within the study area (bounded by 15°-20°N and 65°-70°W) for 102 years reveals only two hurricanes having a forward speed of 22 knots (estimated from 24-hr positions) during the period of 1871 through 1972, thus Figure 3-4 is in general representative of the longer period.

3.7 Frequency of Tropical Cyclone Tracks

The tide frequency analysis treats three classes of storms separately, i.e., landfalling, exiting, and alongshore storms, because the dynamic model described in Chapter 4 is set up to handle these separately. It is, therefore, logical to examine frequency of tropical cyclone occurrences separately according to these three predetermined categories, and this was done for the north, west, and south coasts. The count methods are explained in the following paragraphs and are summarized in Table 3-2. The predominant track directions are from the east and ESE (Figure 2-1).

3.7.1 Seaward alongshore storms, San Juan

A north-south line was drawn on a map through San Juan. Tropical cyclone tracks ("hurricanes" plus "tropical storms") crossing this line were counted for the period 1871-1972. Storms that had crossed land east of the line--that is, storms that passed over the northeast corner of the island and then exited the coast--are omitted from the seaward count. The accumulated seaward count is shown in the right half of Figure 3-5. All crossings were from east to west.

3.7.2 Landward alongshore storms, San Juan

Storms that crossed the north-south line through San Juan on the landward side of the city were counted; the accumulated frequency is shown on the left half of Figure 3-5.

3.7.3 Landward alongshore storms, south coast

Storms crossing $66^{\circ}30'$ north of the south coast were counted, with the accumulated frequency for the 102 years shown in the left half of Figure 3-6.

3.7.4 Seaward alongshore storms, south coast

Storms crossing $66^{\circ}30'$ south of the Puerto Rico coast were counted, except those striking the island (on the southwest corner) were omitted. The accumulated count is shown in the right half of Figure 3-6.

3.7.5 Landfalling storms, south coast

The frequency of landfalling storms on the south coast was estimated by the track density method described in the next section. Exiting storms on the south coast are so rare they are neglected.

3.7.6 Exiting storms, north coast

Since the north and south coasts are essentially parallel and the

north-south gradient of storm frequency is slight, the exiting storm frequency on the north coast was assumed to be the same as the landfalling frequency on the south coast without making any calculations. Landfalling storms on the north coast are neglected.

3.7.7 West coast

"Exiting" storms is the only important category for the west coast. An estimate of the frequency was obtained by averaging the "landward alongshore" frequencies for San Juan and for the south coast.

3.7.8 East coast

No computations were made for the east coast.

3.8 Track density method

The frequency with which hurricane storm tracks landfall on the southern Puerto Rico coast is more complicated than "alongshore" because of the small angle between tracks and coast and the varying coastal directions. In order to handle this in a straightforward manner we resort to the track density method described in this section.

3.8.1 Track frequency

The frequency of occurrence of tropical cyclones may be expressed as storm track density at a point. This is defined as the number of storm tracks which cross that point, from any direction, per unit length normal to track per unit time. In concept, one obtains this number by a limit process which may be expressed as:

$$\lim_{D \rightarrow 0, t \rightarrow \infty} \left(\frac{N}{Dt} \right) = \text{storm track density at a point,}$$

where N is the count of tracks passing through a circle of diameter D in time t. Practically it is necessary to count storm tracks passing through a large enough circle over a long enough period of time to smooth out random fluctuations. This was done by counting tropical cyclone tracks from the sources mentioned earlier over 2.5° longitude squares with the corners cut off to approximate circles.

The number of storms passed through each of these 2.5° "octagons" is shown in Figure 3-7 between 15° and 20°N and 60° and 70°W. These values approximate the number of storms passed through a circle of 150 nautical miles diameter per 102 years. A smoothing analysis of these numbers yields the estimate of "point track density." The adopted count for the southern coast of Puerto Rico, by visual analysis of Figure 3-7, is 49. This is equivalent to 3.2 storms per 10 nautical miles per 100 years:

$$49 \times \frac{10}{150} \times \frac{100}{102} = 3.2$$

3.8.2 Direction probability

The second part of the track density analysis for each 2.5° octagon is the track direction. Track directions by 15° class intervals were counted for the 102 years for each octagon.

Histograms like Figure 3-8 were then constructed for each octagon. The ordinate is the normalized frequency of occurrences (f/Ni), where f is the count in a direction class interval, N the total count for all directions for the octagon and i the class interval width (in degrees). A "Beta" distribution function was then fitted to each of these histograms by using a computer program listed in the "IBM Scientific Subroutine Package."

An accumulated probability curve is obtained by integrating the "Beta" curve. An example of these plots is shown in Figure 3-8.

3.8.3 Application at a point

Finally, the frequency with which storms enter a coast from a particular direction span is a product of the point track density for the region, the fraction of the total storms within the specified direction span, and the sine of the angle between the coast and the storm direction class interval. Example: Given that a portion of the southern coast of Puerto Rico is oriented 90°-270°, the overall track density is 3.2 storms per 10 nautical miles per 100 years and 30% of the storms come from directions between 115° and 135°. (Average direction 125° = 35° to coast.) The computed count of landfalling storms from this direction interval is $3.2 \times .3 \times \sin 35^\circ = .55$ storms per 10 nautical miles of coast per 100 years. Carrying out this operation through 180° gives the total landfalling frequency. The exiting frequency can be handled in the same way.

3.8.4 Landfalling frequency on southern coast

The accumulated direction of motion curve from Figure 3-8 for the Puerto Rico octagon is replotted in Figure 3-9 on a larger scale. Direction of motion between 115° and 200° is construed as "landfalling" for east-west portions of the southern coast. This 50% of the total storms is grouped into the three class intervals shown by the dotted line in the diagram: 125°, 30%; 150°, 18%; 180°, 2%. Applying the procedure in the example above to each class interval in combination with the track density of 3.2 storms per 10 n. mi. per 100 years gives a total landfalling frequency of 1.1 per 10 n. mi. per 100 years.

3.9 Probability distribution of tropical cyclone direction of motion

This is one of the factors required for surge computation for landfalling and exiting storms. It is given by Figure 3-9.

TABLE 3-1
Hurricane Parameters

Storm	Date	Name	CPI (mb)	R (n.mi.)	T (kt)	max. wind (kt)	eye diam. (n.mi.)	Reference point	
								Lat °N	Long °W
1947	Sep 4-21	--	952	--	15	120	7	22.3	66.6
1950	Aug 20-Sep 1	BAKER	990	8	11	90	12	17.1	61.0
1950	Aug 30-Sep 16	DOG	962	18	10	120	20	19.6	64.4
1951	Aug 12-23	CHARLIE	978	--	22	90	22	16.5	72.9
1953	Aug 28-Sep 9	CAROL	929	11	16	130	3	19.8	60.4
1955	Aug 3-14	CONNIE	952	12	16	120	20	19.5	63.7
1956	Aug 9-19	RETSY	973	14	16	108	16	17.9	66.1
		(after Colón)							
1958	Aug 30-Sep 6	ELLA	983	20	16	95	30	16.8	70.5
1958	Sep 4-12	FIFI	1,000	--	16	80	30	19.7	60.9
1960	July 9-16	ABBY	992	8	15	85	15	14.6	65.7
1960	Aug 29-Sep 13	DONNA	942	13	13	140	22	16.9	60.0
1963	Sep 23-29	EDITH	978	--	10	110	25	14.7	62.8
		(after Dunn and Miller)							
1963	Sep 26-Oct 13	FLORA	954	10	9	130	20	15.5	70.7
1964	Aug 20-Sep 5	CLEO	938	6	15	135	12	16.8	66.7
1966	Aug 21-Sep 5	FAITH	987	15	15	98	10	19.9	65.2
1966	Sep 21-Oct 11	INEZ	932	4	14	140	8	16.9	66.6
1967	Sep 5-22	BEULAH	940	12	8	126	10	16.7	66.7

TABLE 3-2

SUMMARY OF TROPICAL CYCLONE TRACK COUNT PROCEDURES
PUERTO RICO, 1871-1972

	Landfalling Storms	Exiting Storms	Alongshore Storms	
			Seaward	Landward
South Coast	"Track density" method.	Omit	Count tracks that miss island crossing 66° 30'W.	Count all tracks that cross 66° 30'W.
North Coast	Omit	"Track density" method (Same count as "land-falling" on south coast.)	Count tracks that miss island crossing north-south line through San Juan.	Count all tracks that cross north-south line through San Juan.
West Coast	Omit	Take average of "landward alongshore" count for north and south coasts.	Omit	Omit

CHAPTER 4

THE HURRICANE SURGE MODEL

4.1 The model

A hydrodynamic model developed by the National Weather Service [8, 9, 10] for the predicting of hurricane surges on the United States mainland coast when a storm is approaching has been employed in all previous coastal flooding frequency reports for the FIA by NOAA. This model computes a complete surface wind-field for the hurricane from the central pressure and the radius of maximum winds. The asymmetry associated with forward motion of the storm is also taken into account. The resulting wind stress on the water, and, by application of the appropriate physical equations of motion, the rise of water level on the Continental Shelf and the coast as the hurricane approaches or passes are then computed. The excitation of a wave by the hydrostatic rise of water level due to the diminution of the overlying atmospheric pressure is also taken into account. To accomplish this, calculations of the requisite physical variables are made at a series of grid points at successive short time intervals. The necessary approximations are made to reduce the computation to a quantity that is economical on a large fast computer.

Computed coastal surges have been compared to observed surges in those hurricanes where sufficient data are available. These comparisons are described in the cited reports. Some of the peculiar conditions confronting the use of this model for the island of Puerto Rico and the approximations to take care of them for the purposes of this study are enumerated below.

4.2 Application of model to Puerto Rico

The hurricane surge program* was modified to handle the island of Puerto Rico. Two main problems were encountered which required fundamental changes and development of the dynamic model; these are: (1) hurricanes along Puerto Rico coasts are smaller than along the Gulf and East Coasts of the United States (2) the slope of the continental shelf at Puerto Rico is steep.

* Known as the "SPLASH" program from the acronym of the publication describing it [9].

The grid spacing in SPLASH is too coarse to see the driving forces of small sized storms; hence, the program was modified to shorten grid length from 4 miles to 2.5 miles; this reduction of grid size required a corresponding reduction of the time step for finite-difference computations and the program is more expensive to run.

The problem of steep shelf slope is more difficult to solve. The approach was empirical. Experiments were performed to arrive at an optimum slope (as close as possible to the real slope) before the computations became unstable. These experiments were time consuming and were a significant portion of the development work required for the Puerto Rico project. Results appear to show that the coastal surge is insensitive to further increases in shelf steepness beyond a certain value.

The modified SPLASH program was run with one-dimensional depth basins for the southern part of Puerto Rico; each basin's depth profile was localized for particular point along the coast. A modified shoaling curve for the southern part of the island was derived. The shoaling curve, with the hurricane climatology for Puerto Rico, described in Chapter 3, was used to estimate surge levels as described in Chapter 5.

On the north coast, where the shelf slope is relatively uniform (Figure 1-1), the slope at San Juan was developed as an example for that area.

CHAPTER 5

STORM TIDE FREQUENCIES BY JOINT PROBABILITY METHOD

5.1 Example--San Juan

The first step in the joint probability method is to divide the hurricane parameter probability distributions into class intervals and read out the mid-point value for each class interval. This is done in Table 5-1. Under forward speed, f , for example, in Table 5-1A, 8 kt. is the mid-point of the lowest 10% of storms from Figure 3-4, 10.9 kt. is the mid-point of the next 20%, etc. Central pressure depression, D , (1011 mb minus central pressure) and direction of motion, θ_L , are similarly abstracted from Figures 3-1 and 3-9.

The radius of maximum winds in Table 5-1A needs additional explanation. Following the precedent of indications of hurricane behavior in the vicinity of Florida and the Gulf of Mexico, some tendency is assumed for smaller radius of maximum winds to be associated with the deepest hurricanes. Thus, in Table 5-1A, 70% of the deepest hurricanes are assumed to have an R of 10 n. mi. and 30% 16.5 n. mi. with a trend toward 50% each for the less intense hurricanes as indicated in the table.

Thus, Table 5-1A defines 288 different hurricanes ($8 \times 2 \times 6 \times 3 = 288$) that in the aggregate represent the climatological possibilities in the vicinity of San Juan. The probability (fraction of all hurricanes) of each of these is obtained by multiplying the respective parameter probabilities in the table. The sum of the probabilities of the 288 hurricanes, of course, equals 1.0. It has already been determined that the frequency of all exiting storms is .0011 per nautical mile of coast per year.

As the second step, calculations are made with the modified SPLASH program described in Chapter 4 of the surge profile that would be produced in the vicinity of San Juan by each of the 288 exiting hurricanes, for the shelf slope specified for that region. (Many of the surge profiles are obtained by adjustment of other profiles rather than by complete surge computer computations.) Then low astronomical tide, high tide, and two intermediate tide levels are added to each of the 288 surge profiles, yielding $4 \times 288 = 1152$ storm tide profiles. (The mean tide range at San Juan is 1.1 feet.) Next, each storm is allowed to exit from the coast not only at the point most critical for San Juan but at points to the east and west, and the storm tide profiles shifted along the coast accordingly.

As the third step, storm tides were similarly computed for the alongshore storms from the data in Table 5-1B. Close in alongshore storms account for more than two-thirds of the tides equal to or exceeding the 100-year value.

Finally, summing all the possibilities--including combination of surges with high, low, and intermediate astronomical tide and coastal placement--yields the total tide frequency graph of Figure 5-1. In working out the joint probability of each hypothesized storm event, D , f , θ_L , astronomical tide, and coastal placement are considered statistically independent, while R is dependent on D as shown in the table. These frequency values are still-water levels on the open coast that would be measured in a tide gauge house or other enclosure, excluding wave action. The wave question is discussed in the next chapter.

5.2 West Coast

The same procedure was used at Mayaguez on the west coast using exiting storms only. The results are compared with San Juan in Figure 5-2. At Mayaguez, being in the lee of the island, the hurricane wind intensity threat is less than at San Juan, but the slope of the sea bottom is not as steep and, therefore, is more critical for production of surges. These factors combine to give the same 100-year return period tide level at Mayaguez as at San Juan, a higher 500-year tide level, and a lower 10-year tide level.

5.3 South Coast

The same procedure was followed at Cabo Robo, Mar Negro, and Playa De Humacao on the south coast for landfalling and alongshore hurricanes with the parameters listed in Table 5-2. The results are shown in Figure 5-3 for the 10-, 25-, 100- and 500-year return periods. Interpolations were then made between these three points following the shoaling factor curve that had been worked out (Chapter 4) from comparative surge calculations with standard hurricanes every few miles along the coast.

5.4 Extrapolation to Uncharted Areas

The objective of this study is to establish the 100-year flood line. A complete tide frequency distribution has been calculated as described for the southern coast of Puerto Rico and selected points on the west and north coasts. The 100-year tide level was interpolated between these points from inspection of water depth maps. This interpolation is shown by the dashed lines on Figures 5-2 and 5-3. In a definitive "type 15" study additional calculations should be made.

5.5 Pressure-wind relationship

Part of the process of computing a hurricane surge from hurricane parameters by the SPLASH program [9] is to calculate the wind field from the three parameters central pressure depression, radius of maximum winds, and one-half the storm motion vector. The theory and empirical relations for doing this are described in [8] and [10]. The stress of wind on water at each grid point at each time step is then obtained by multiplying the wind vector by a stress coefficient.

It turns out that the maximum hurricane wind speeds calculated by this method are consistently smaller than the maximum wind speed estimates from aircraft for the hurricanes in Table 3-1. The latter are presumed to be estimates of the surface wind derived from the appearance of the sea as seen from the aircraft and from the measured wind at flight level.

The maximum wind speeds computed by the SPLASH program, using an average storm forward speed of 14 knots, and the aircraft-reported maximum winds are both plotted vs. central pressure for this set of hurricanes in Figure 5-4. Curves are fitted by eye to the two sets of points.

For this study we have adhered to the results given by the current version of the SPLASH computer program. The disparity between the two wind-pressure relations in Figure 5-4 is large enough that in a "type 15" study for Puerto Rico the pressure-wind relationship for that region should be reexamined. Such a reexamination would involve the total system, including the atmospheric frictional coefficients which are used in computing the surface wind field dynamically and the wind-on-water stress coefficient.

We note one precedent for a disparity between aircraft hurricane winds and winds from other sources in the Caribbean area being resolved in favor of the other sources. Reference [11] contains an analysis of the surface wind field in hurricane HAZEL of 1954 in the vicinity of Great Inagua Island, p. 93 and Figure 12-5 of the report. Ship reports and indirect calculations were given more weight than aircraft reconnaissance reports.

TABLE 5-1

Tropical Storm Parameters--San Juan, Puerto Rico

A.

Exiting Storms							
$F_e = .0011$							
D	P_i	Prd		f	P_f	θ_L	P_θ
		R=10	R=16.5				
85.0	0.01	0.7	0.3				
79.2	.03	.7	.3	8.0	0.1		
71.1	.06	.6	.4	10.9	.2	35	0.60
60.3	.10	.6	.4	13.9	.2	60	.36
43.2	.20	.5	.5	15.3	.2	90	.04
25.2	.20	.5	.5	16.4	.2		
14.4	.20	.5	.5	20.6	.1		
9.0	.20	.5	.5				

B.

Alongshore Storms				
L	F_b (at sea)	F_b (inland)	R	P_r
2.0	0.0098	0.0118		
6.5	.0118	.0118		
11.0	.0118	.0108	10.0	0.5
15.0	.0118	.0108	16.5	.5
21.7	.0275	.0186		
30.4	.0304	.0196		

Symbols are identified on page 21.

TABLE 5-2

Tropical Storm Parameters--South Coast, Puerto Rico

A.

Landfalling Storms							
$F_n = .0011$							
D	P_i	Prd		f	P_f	θ_L	P_θ
		R=10	R=16.5				
94.0	0.01	0.7	0.3				
88.0	.03	.7	.3	8.0	0.1		
79.0	.06	.6	.4	10.9	.2	35	0.60
67.0	.10	.6	.4	13.9	.2	60	.36
48.2	.20	.5	.5	15.3	.2	90	.04
28.0	.20	.5	.5	16.4	.2		
15.6	.20	.5	.5	20.6	.1		
10.0	.20	.5	.5				

B.

Alongshore Storms				
L	F_b (at sea)	F_b (inland)	R	P_r
4.3	0.0186	0.0079		
13.0	.0205	.0088		
21.7	.0235	.0127	10.0	0.5
30.4	.0254	.0137	16.5	.5
39.1	.0274	.0147		
47.8	.0314	.0157		

Symbols are identified on page 21.

Legend for Tables 5-1 and 5-2

- D = Central pressure deficit (mb).
- P_i = Proportion of total storms with indicated D value.
- f = Forward speed of storm (knots).
- P_f = Proportion of total storms with indicated f value.
- R = Distance from center of storm to principal belt of maximum winds (nautical miles).
- P_r = Proportion of storms with indicated R value.
- P_{rd} = Proportion of storms in D class with indicated value.
- θ_L = Direction of entry, measured clockwise from the coast (degrees).
- P_θ = Proportion of total storms with indicated θ_L value.
- L = Effective distance perpendicularly landward or seaward from coast to storm track (nautical miles).
- F_b = Average number of storms per year that pass at distance L.
- F_n, F_e = Frequency of storm tracks crossing coast, landfalling and exiting, respectively (storm tracks per nautical mile of coast per year).

Notes: (1) Alongshore storms have the same values of D, P_i , f, and P_f as those for landfalling.

CHAPTER 6

WAVE EFFECTS

6.1 Introduction

Hurricanes as well as winter-type extra-tropical cyclonic wind storms produce high waves. The pounding of breaking waves is responsible for much of the beach erosion and structure damage on the immediate beach front in storms. Near the coast wave amplitudes (trough to crest) are restricted by physical constraints to about 0.7 of the water depth. The Corps of Engineers, Department of the Army, is making a study of wave height criteria for coastal flood insurance analyses for the FIA. In tidal flood mapping to date, pending results of this study, a "velocity zone" has been delineated by NOAA and other agencies along the beach front where serious wave damage can occur, with the inland limits of this zone estimated subjectively by reference to terrain.

6.2 Wave problem in Puerto Rico

For several reasons, the wave question is particularly critical in assessing the coastal flood hazard in Puerto Rico. First, much of the coastline is relatively steep and the zone subject to inundation is narrow. In some areas the entire flood zone can be reached by waves. Second, the slope of the sea bottom from the shore outward is relatively steep. The effect of this is to limit surge levels, which are highest in shallow water, but to expose the beach to large waves. As already mentioned, the limiting factor on wave height, once equilibrium with wind force is reached, is water depth. Third, the long fetch of open water in almost every direction from the island allows storms to impose a full measure of wave-generating energy on the sea.

6.3 Wave swash study for extratropical storms

Fields and Jordan of the U.S. Geological Survey have surveyed and analyzed wave damage on the north coast of Puerto Rico [12] in a cooperative study with the Department of Public Works, Commonwealth of Puerto Rico. Their data deal with extra-tropical (winter) storm events during the 1960's. In each instance storms far to the north (north of Bermuda) produced swells resulting in severe waves on the north coast. Their report [12] shows maps of "wave swash" elevations (height of water on the coast in waves) in the December 4, 1967 storm, which destroyed more than 300 beach-front homes between

San Juan and Arecibo. Figure 6-1 is a reprint of their tentative wave swash stage-frequency relation for Arecibo and Figure 6-2 a reprint of their generalized diagram. The report gives specific data on the decrease of wave height inland and up river courses, which is rapid.

6.4 Estimated hurricane effects

Strong hurricanes passing north of Puerto Rico could be expected to produce waves comparable to those described in [12]. Hurricanes have stronger winds but shorter fetch and usually persist less time in a given location than the worst wave-producing extra-tropical storms.

The south coast of Puerto Rico is not exposed to waves from extra-tropical cyclones to any important degree. Waves can be expected in hurricanes. On a frequency basis waves of a given amplitude will occur less frequently on the south coast than on the north coast but may occur in combination with higher surges.

CHAPTER 7

DEMARCATIION OF FLOOD PRONE LIMITS

7.1 Objective

The objective of this study is to indicate the approximate limit of special flood hazards along the coast of Puerto Rico on maps for the Federal Insurance Administration. This limit has been delineated directly on existing USGS topographic quadrangles without field surveys. (Field surveys would be necessary for a "type 15" study.) Principal guidelines for this, besides the topography, are the derived 100-year hurricane tide levels (Figures 5-2 and 5-3) and the wave swash analysis in [12].

7.2 Precipitous coastal areas

In the application of these factors, terrain plays an important role. Much of the coast of Puerto Rico is precipitous. In such areas to delineate the inland limit of flooding, an estimate for wave swash was added directly to the 100-year hurricane tide level. Reference [12] served as a guide for the swash estimates, using the higher values cited. This presupposes that waves associated with hurricanes on both the north and south coasts could be comparable to the more severe wave swash events described in [12]. The latter are from extra-tropical storms.

7.3 Flat coastal areas

For the flatter flood plain areas it was assumed that waves would be damped out a short distance inland. The figures and maps in [12] served as a guide for estimating the inland penetration of the wave swash. Beyond this wave penetration zone, the hurricane 100-year tide level controlled the inland limit of special flood hazard. In coastal reaches intermediate between precipitous and nearly flat, intermediate criteria were applied: the hurricane tide level plus a modest increment for wave swash.

REFERENCES

1. Colón, José A., "Meteorological Conditions over Puerto Rico during Hurricane Betsy, 1956," Monthly Weather Review, Vol. 87, No. 2, February 1959, pp. 69-80.
2. Cry, George W., "Tropical Cyclones of the North Atlantic Ocean," Technical Paper No. 55, U.S. Weather Bureau, Washington, D.C., 1965, 148 pp.
3. U.S. Fleet Weather Facility, "Annual Tropical Storm Report," Jacksonville and Miami Florida, 1945-1972.
4. Dunn, Gordon E., and Miller, Banner I., Atlantic Hurricanes, Louisiana State University Press, Baton Rouge, La., 1964, 377 pp.
5. Myers, Vance A., "Joint Probability of Tide Frequency Analysis Applied to Atlantic City and Long Beach Island, N.J.," ESSA Technical Memorandum WBTM HYDRO 11, Environmental Science Services Administration, Silver Spring, Md., April 1970, 109 pp.
6. Ho, Francis P., Goodyear, Hugo V., and Schwerdt, Richard W., "Some Aspects of Climatological Characteristics of Hurricanes and Tropical Storms, Gulf and East Coasts of the United States," (paper presented at the Eighth Technical Conference on Hurricanes and Tropical Meteorology of the American Meteorological Society, Key Biscayne, Florida, May 1973, to be published).
7. Shea, Dennis J., "The Structure and Dynamics of the Hurricane's Inner Core Region," Atmospheric Science Paper No. 182, Department of Atmospheric Science, Colorado State University, Fort Collins, Colorado, April 1972, 134 pp.
8. Jelesnianski, Chester P., "Numerical Computations of Storm Surges With Bottom Stress," Monthly Weather Review, Vol. 95, No. 11, November 1967, pp. 740-756.
9. Jelesnianski, Chester P., "SPLASH (Special Program To List Amplitudes of Surges From Hurricanes) I. Landfall Storms," NOAA Technical Memorandum NWS TDL-46, National Oceanic and Atmospheric Administration, Silver Spring, Md., April 1972, 52 pp.
10. Jelesnianski, Chester, and Taylor, A.D., "A Preliminary View of Storm Surges Before and After Storm Modifications," NOAA Technical Memorandum ERL WMPO-3, National Oceanic and Atmospheric Administration, Boulder, Colorado, May 1973, 33 pp.
11. Graham, Howard E., and Hudson, Georgina N., "Surface Winds Near the Center of Hurricanes (and Other Cyclones)," National Hurricane Research Project, Report No. 39, U.S. Weather Bureau, Washington, D.C., September 1960, 200 pp.
12. Fields, Fred K., and Jordon, Donald G., "Storm-Wave Swash Along the North Coast of Puerto Rico," Hydrologic Investigations Atlas HA-430, U.S. Geological Survey, Washington, D.C., 1972.

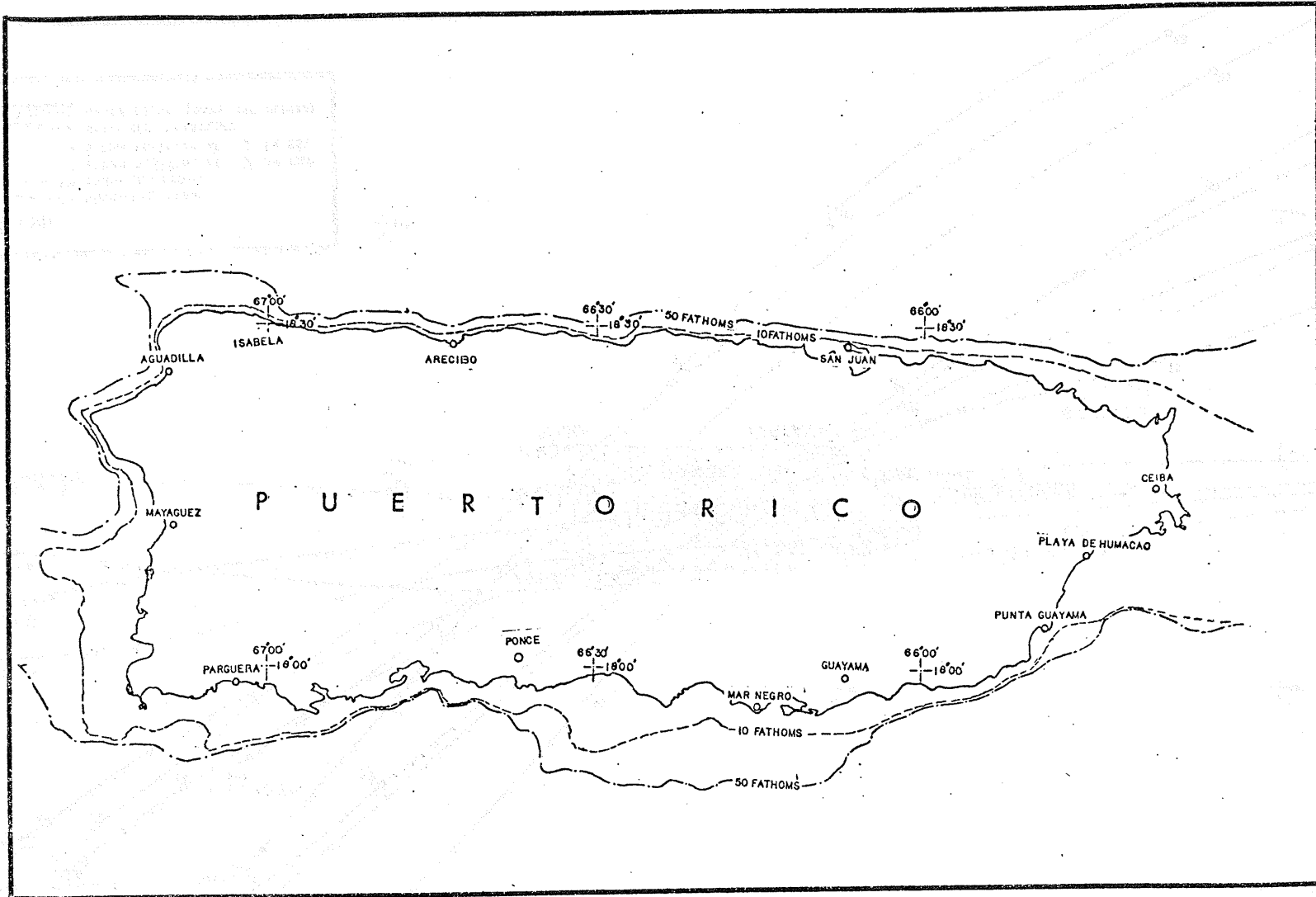


Figure 1-1. --Locator map.

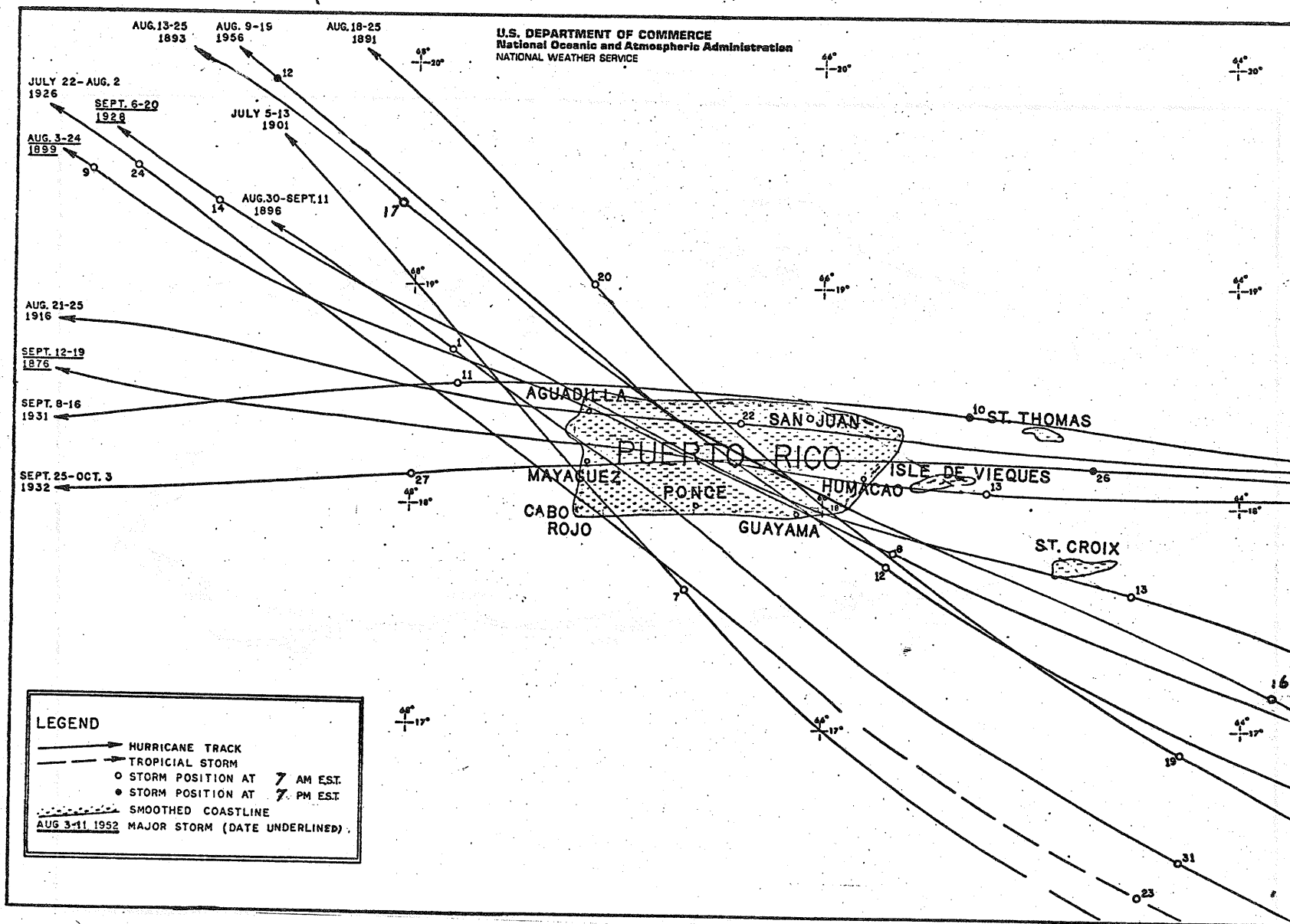


Figure 2-1.-- Landfalling hurricanes for the period 1871-1972.

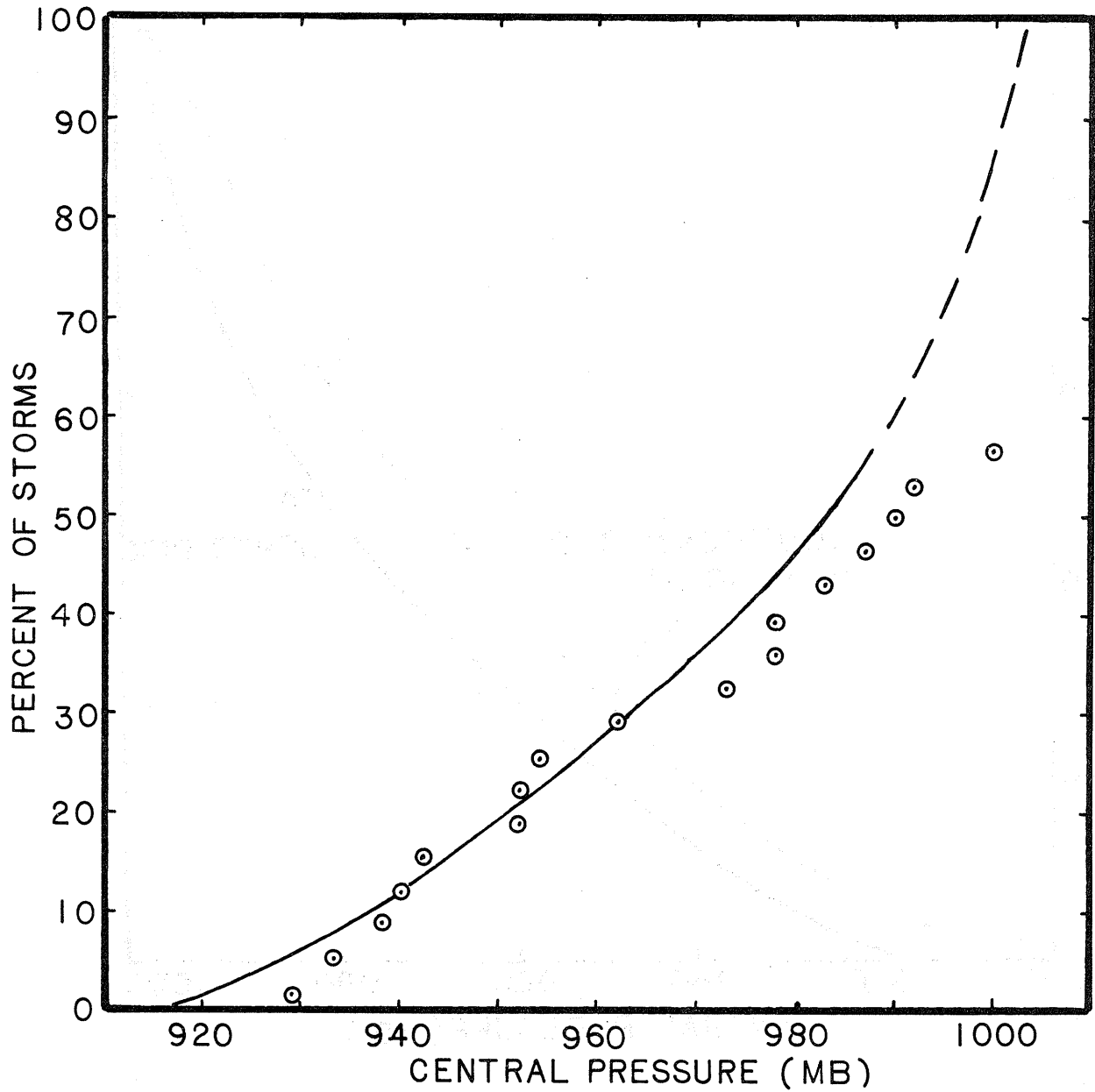


Figure 3-1.--Probability distribution of tropical cyclone central pressure (based on data listed in Table 3-1) in the Puerto Rico area, 1945-1972.

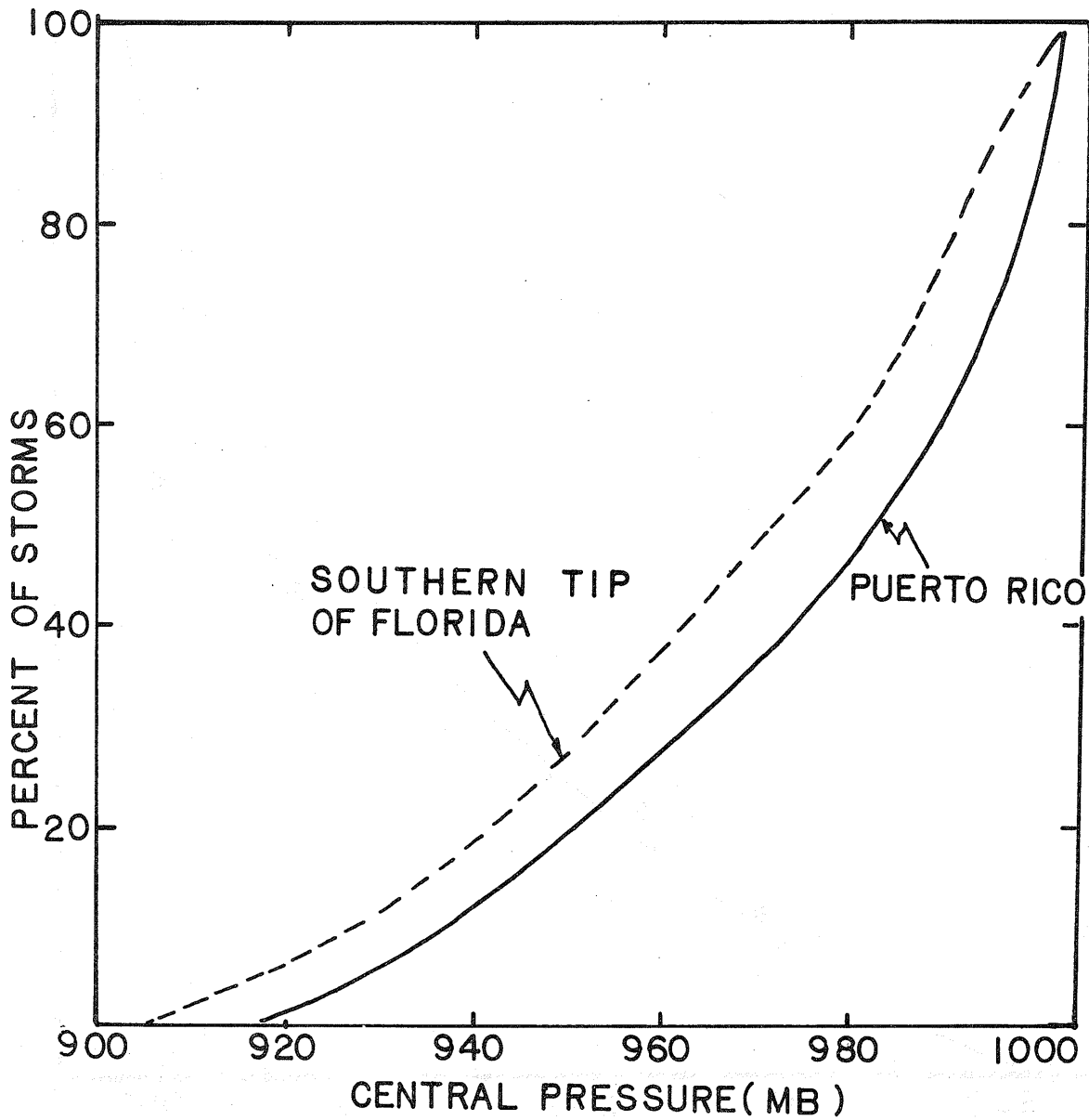


Figure 3-2.--A comparison of probability distributions of tropical cyclone central pressure for Puerto Rico area (18°N) and the southern tip of Florida (25°N).

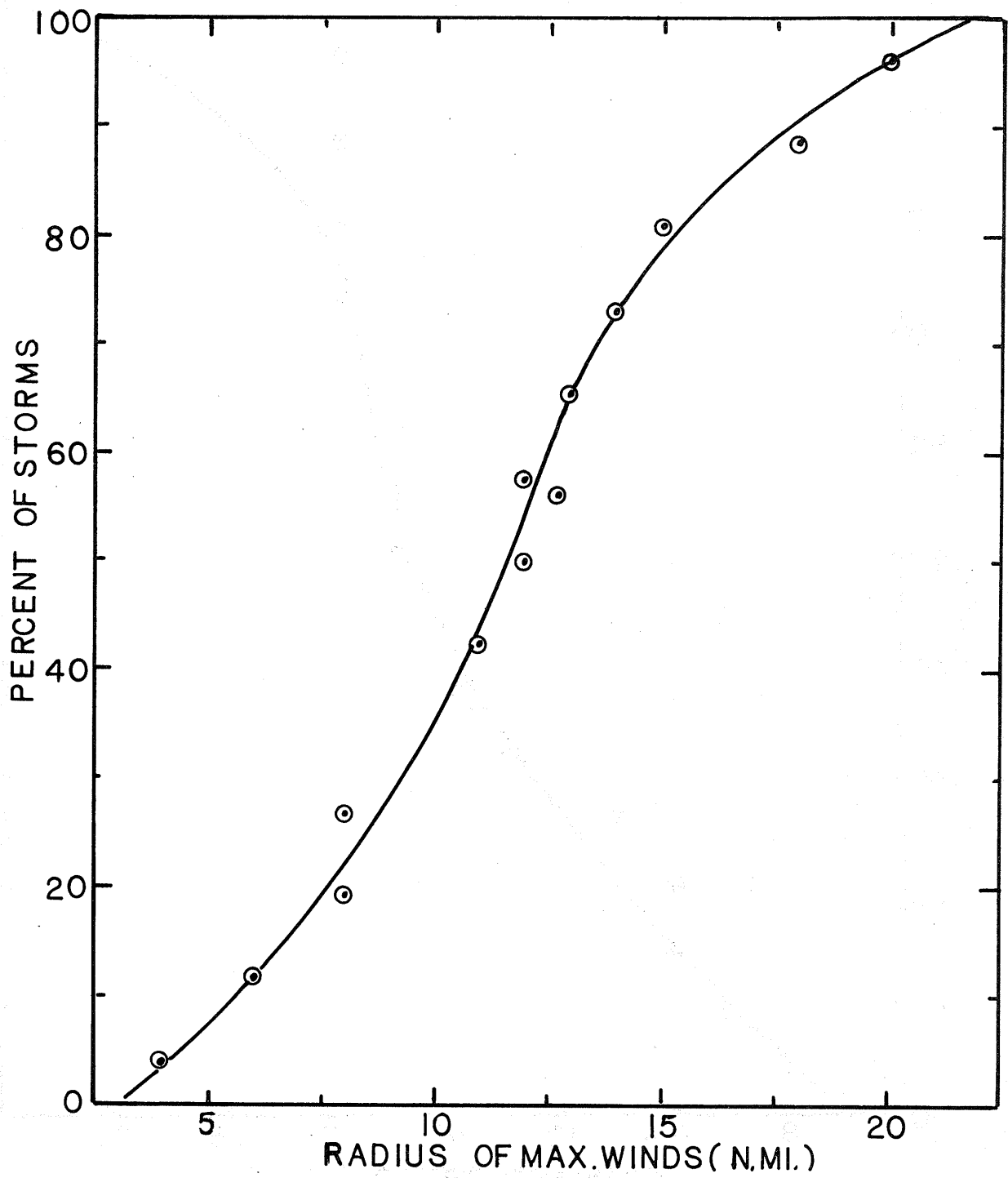


Figure 3-3.--Same as Figure 3-1 but for radius of maximum winds.

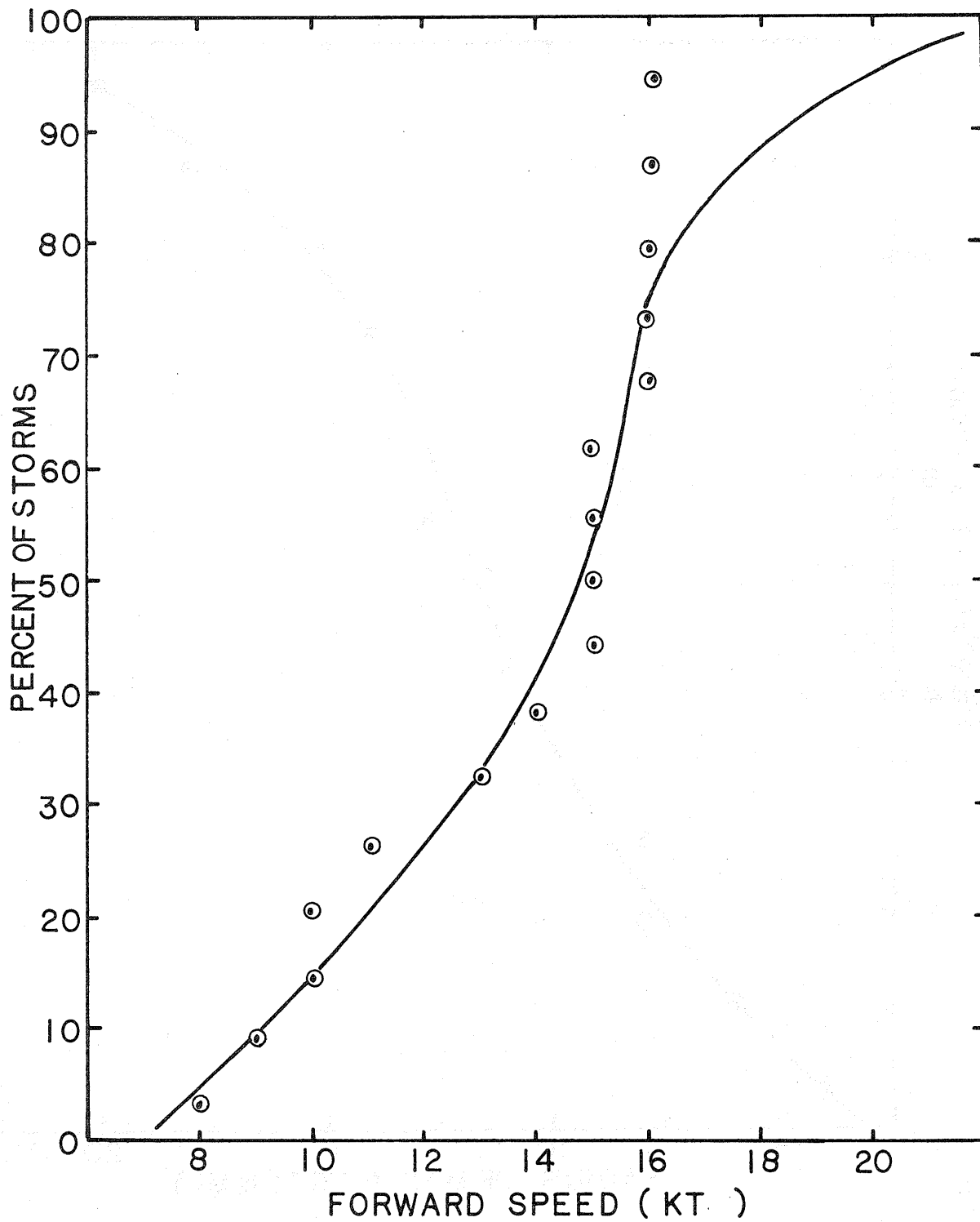


Figure 3-4.--Same as Figure 3-1 but for speed of forward motion.

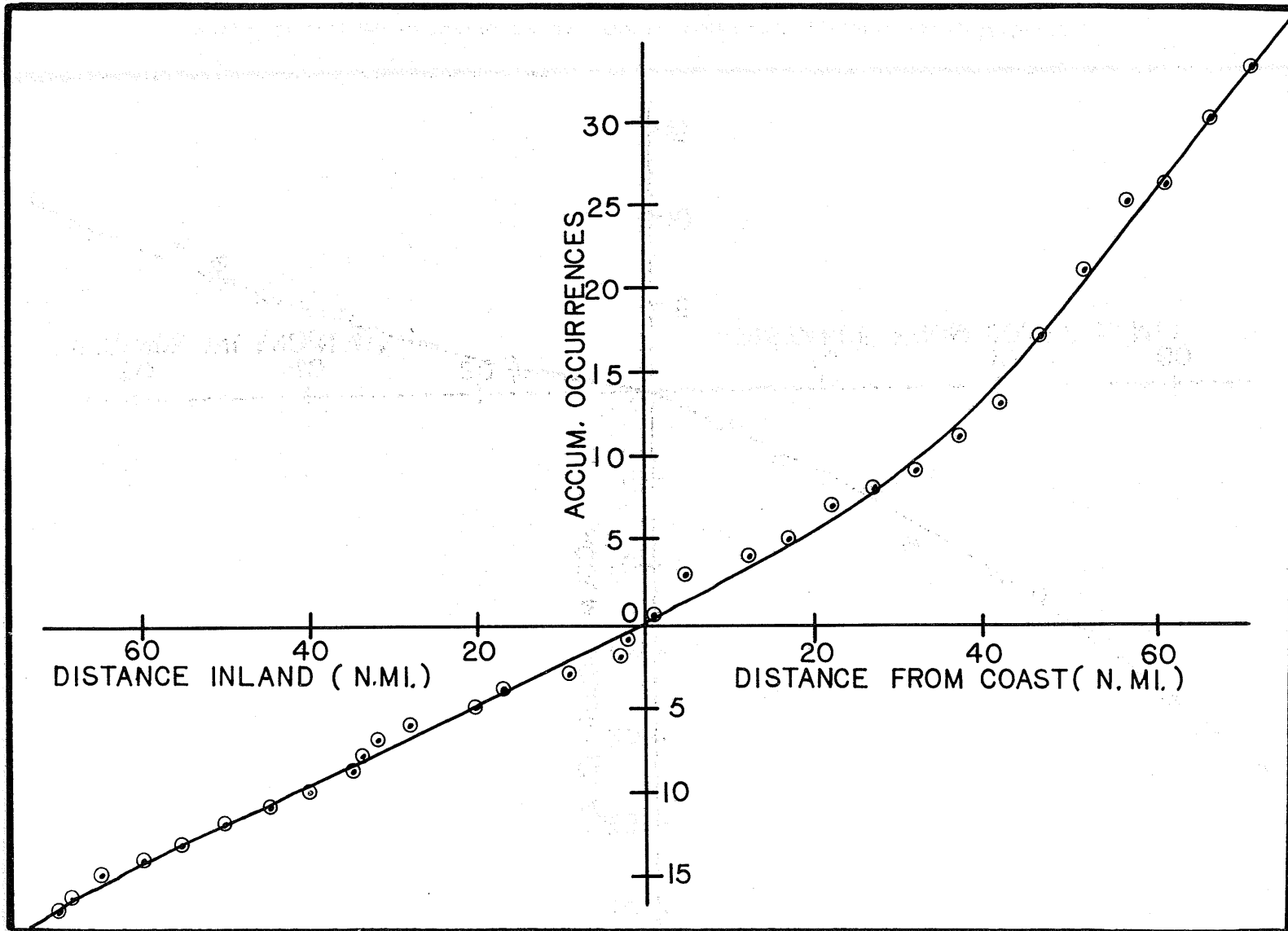


Figure 3-5.--Accumulative frequency of alongshore tropical cyclones for San Juan, Puerto Rico, 1871-1972.

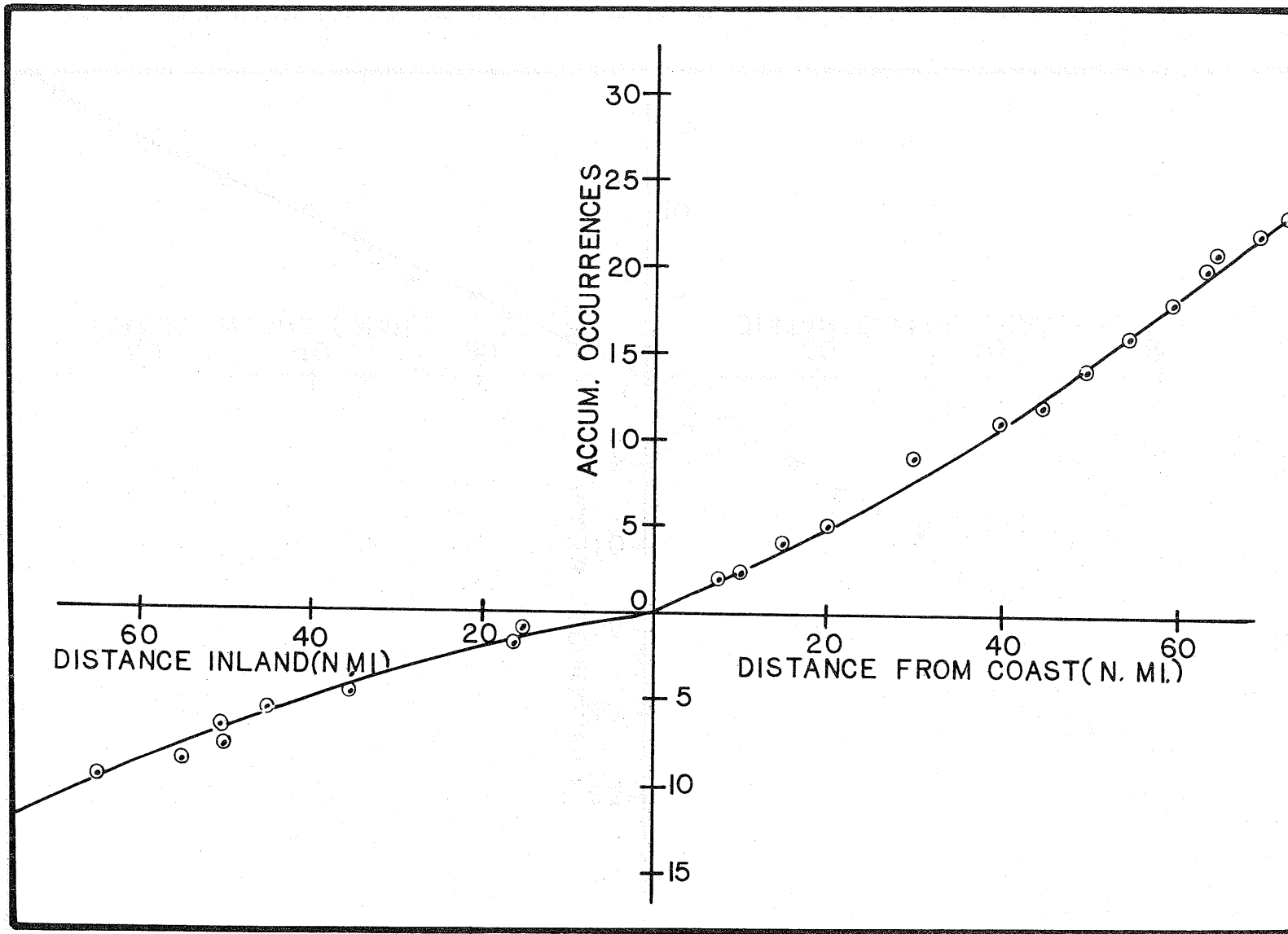


Figure 3-6.--Same as Figure 3-5 but for southern coast, Puerto Rico, 1871-1972.

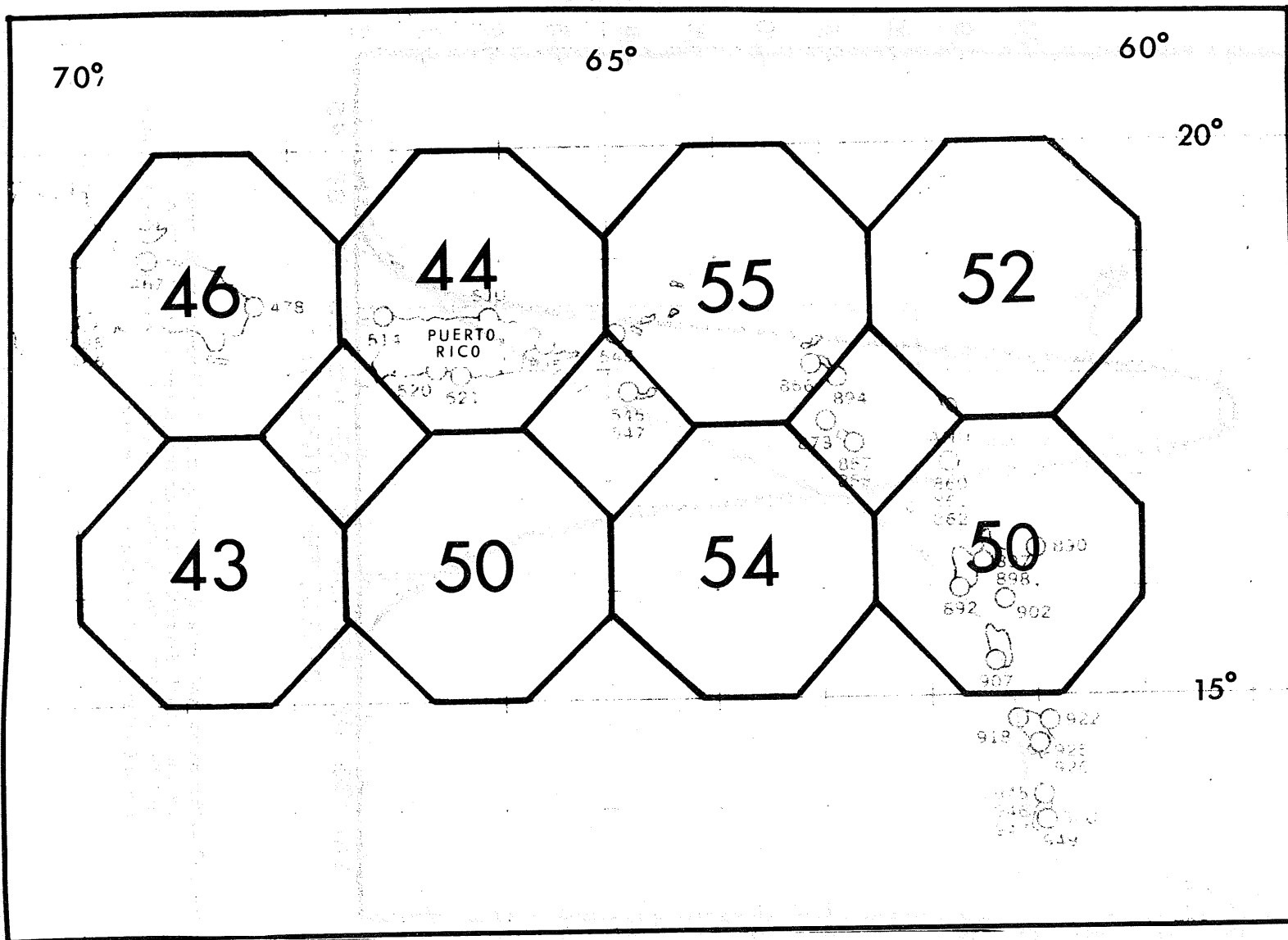


Figure 3-7.--Frequency of tropical cyclone occurrences over 2.5 degree latitude and longitude octagons in the vicinity of Puerto Rico in 102 years. 1871-1972.

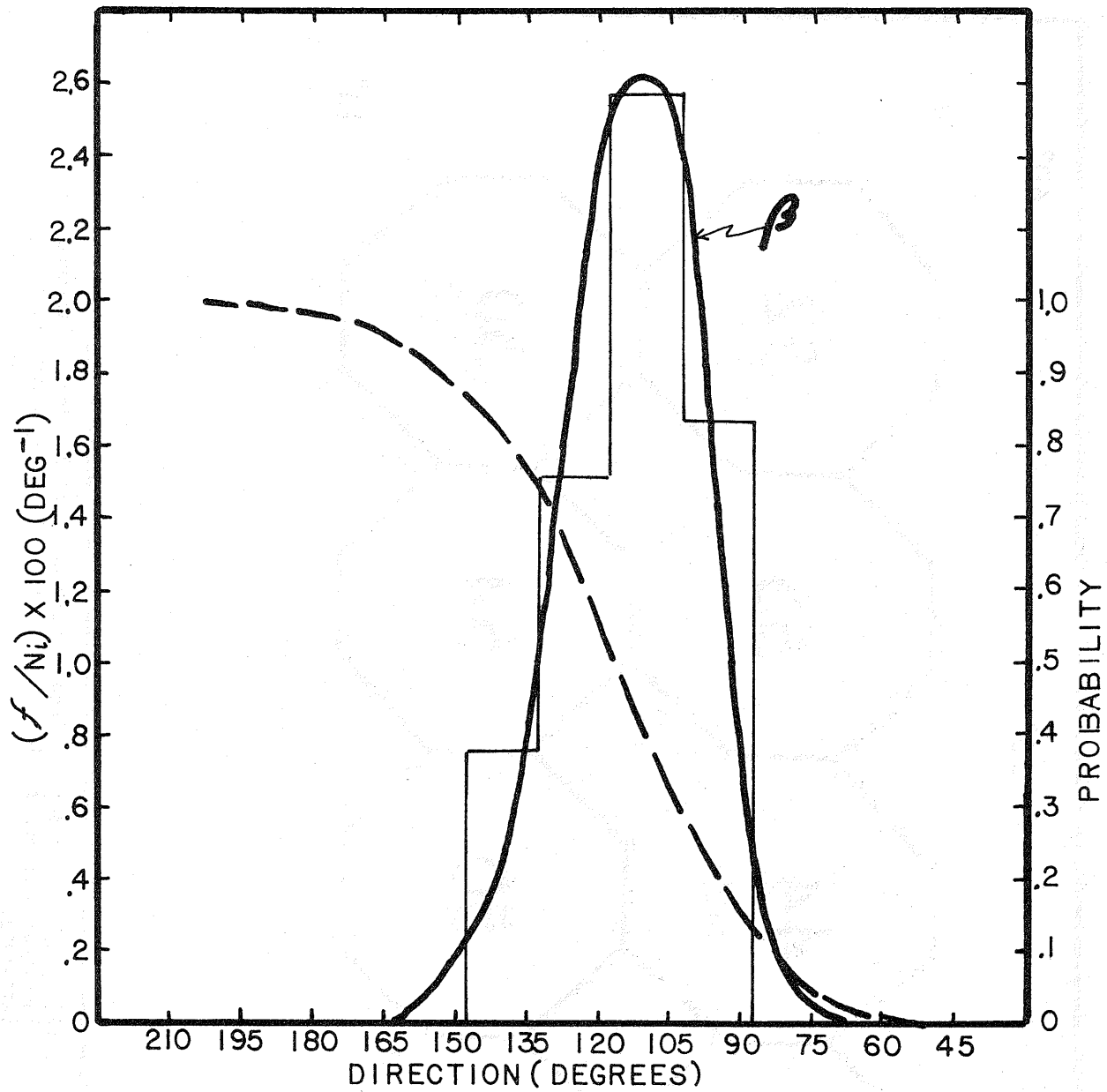


Figure 3-8.--Histogram and Beta distribution fit for frequency of tropical cyclone track direction for octagon bounded by 17.5-20.0°N and 65.0-67.5°W. Dashed line denotes the accumulated probability distribution of direction of storm motion.

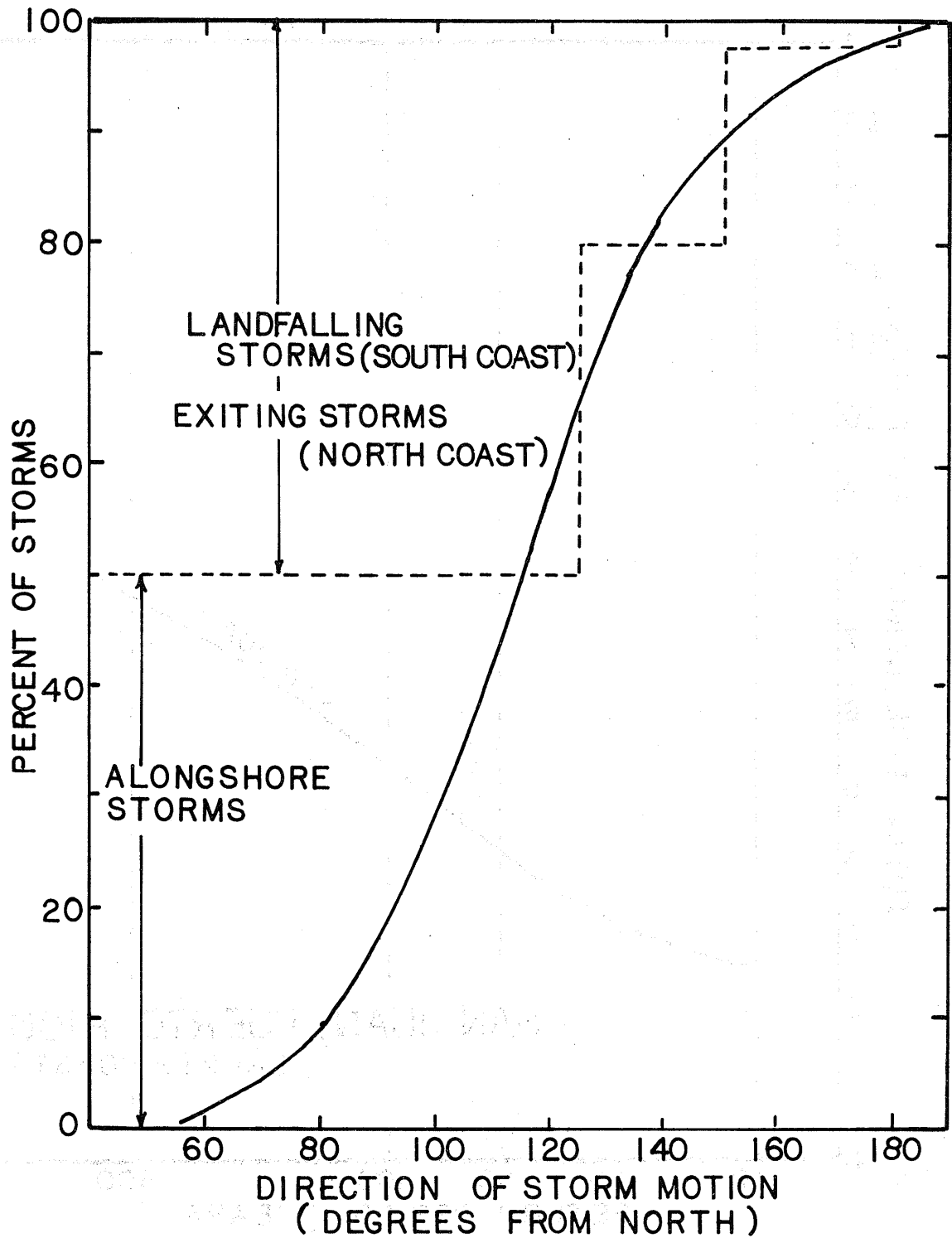
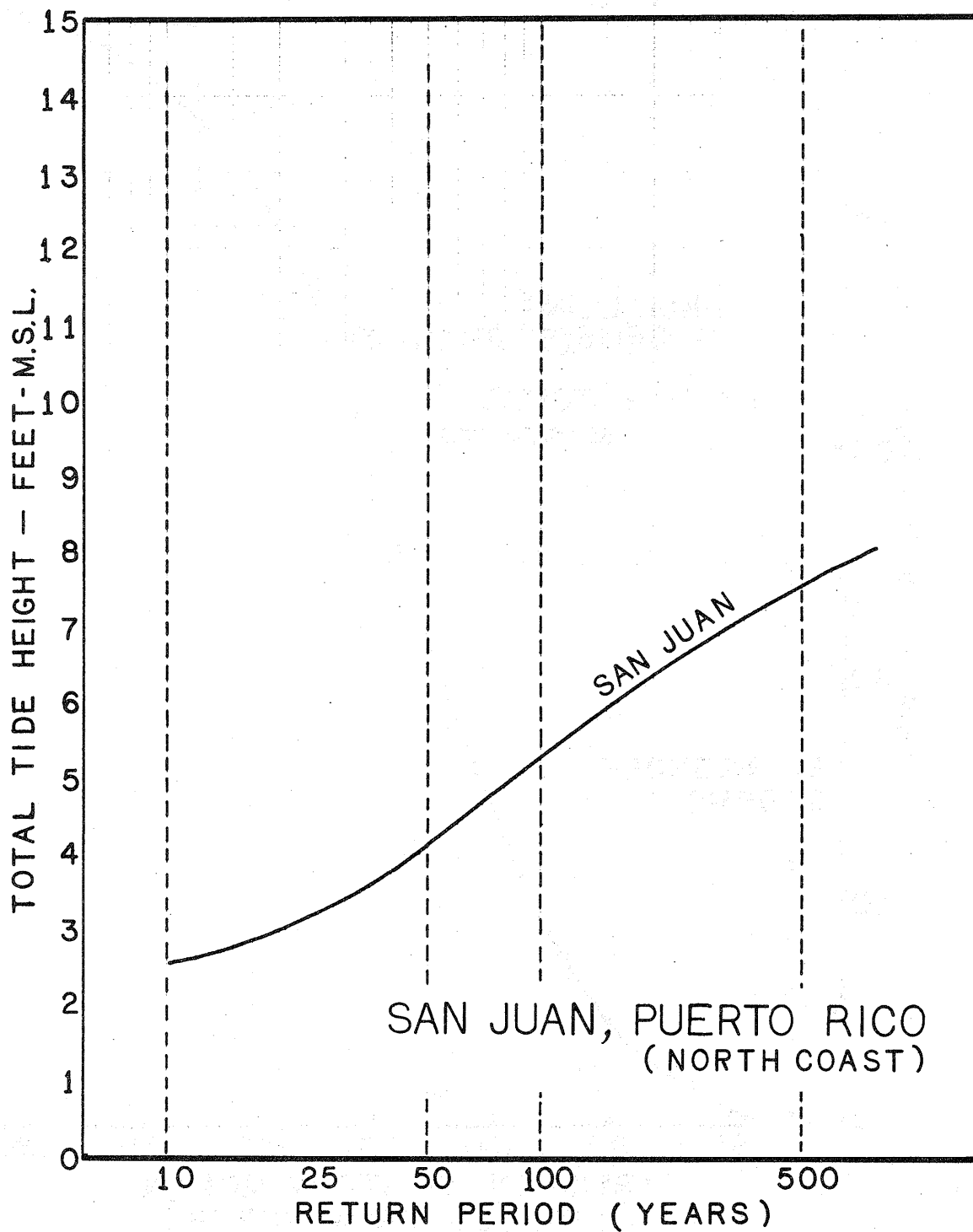


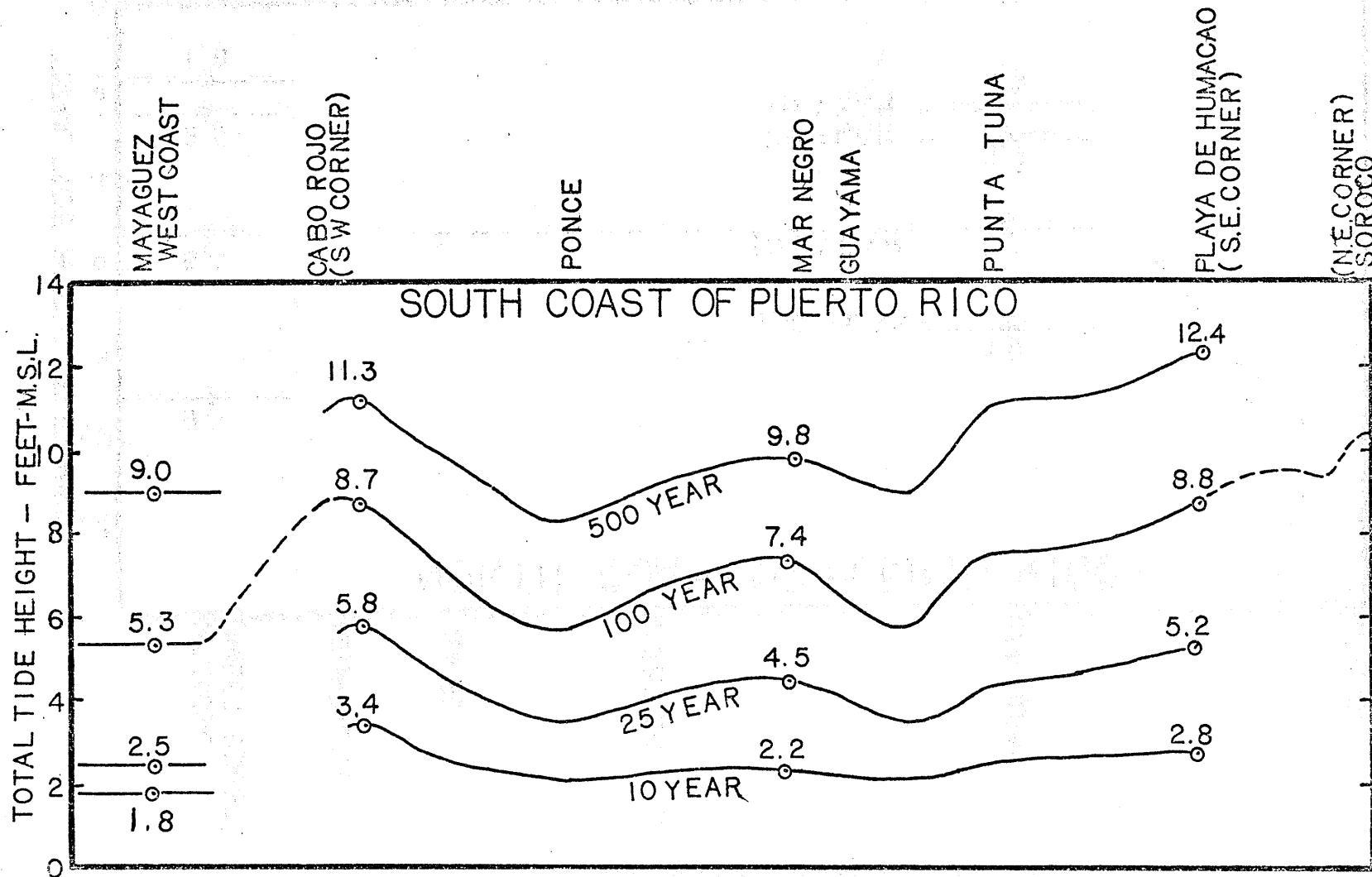
Figure 3-9.-- Accumulative probability distribution of direction of tropical cyclone motion 17.5-20°N 65-67.5°W, from Figure 3-8. Dashed lines denote class intervals adopted for tide frequency computation.



TOTAL TIDE FREQUENCY CURVE

Figure 5-1. -- Tide frequency. San Juan, Puerto Rico.

Figure 5-2.---Interpolated total tide frequency for the 10-, 25-, 100-, and 500-year return period, south coast, Puerto Rico and interpolated 100-year value for west and east coast.



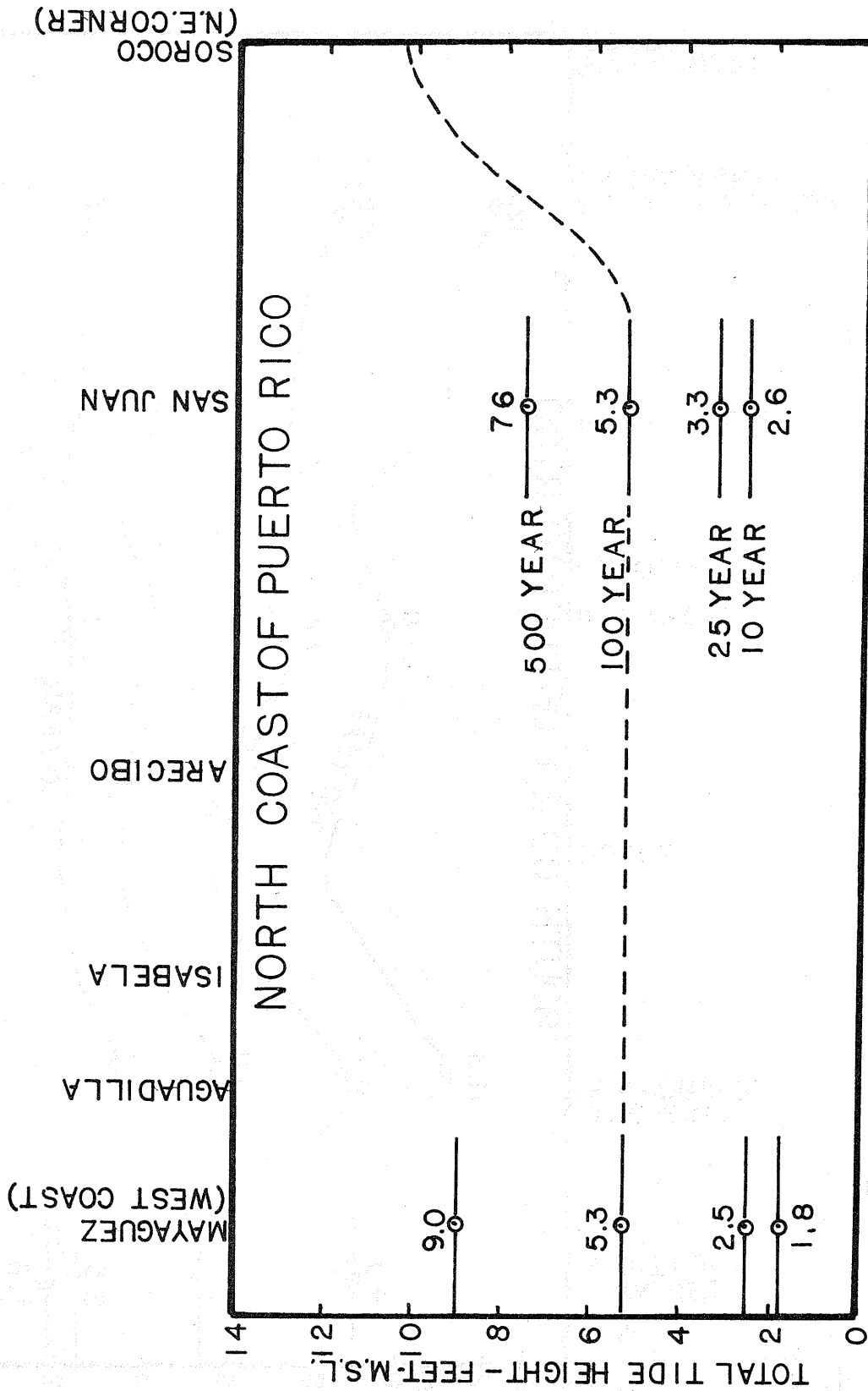


Figure 5-3.--Same as Figure 5-2 for north coast.

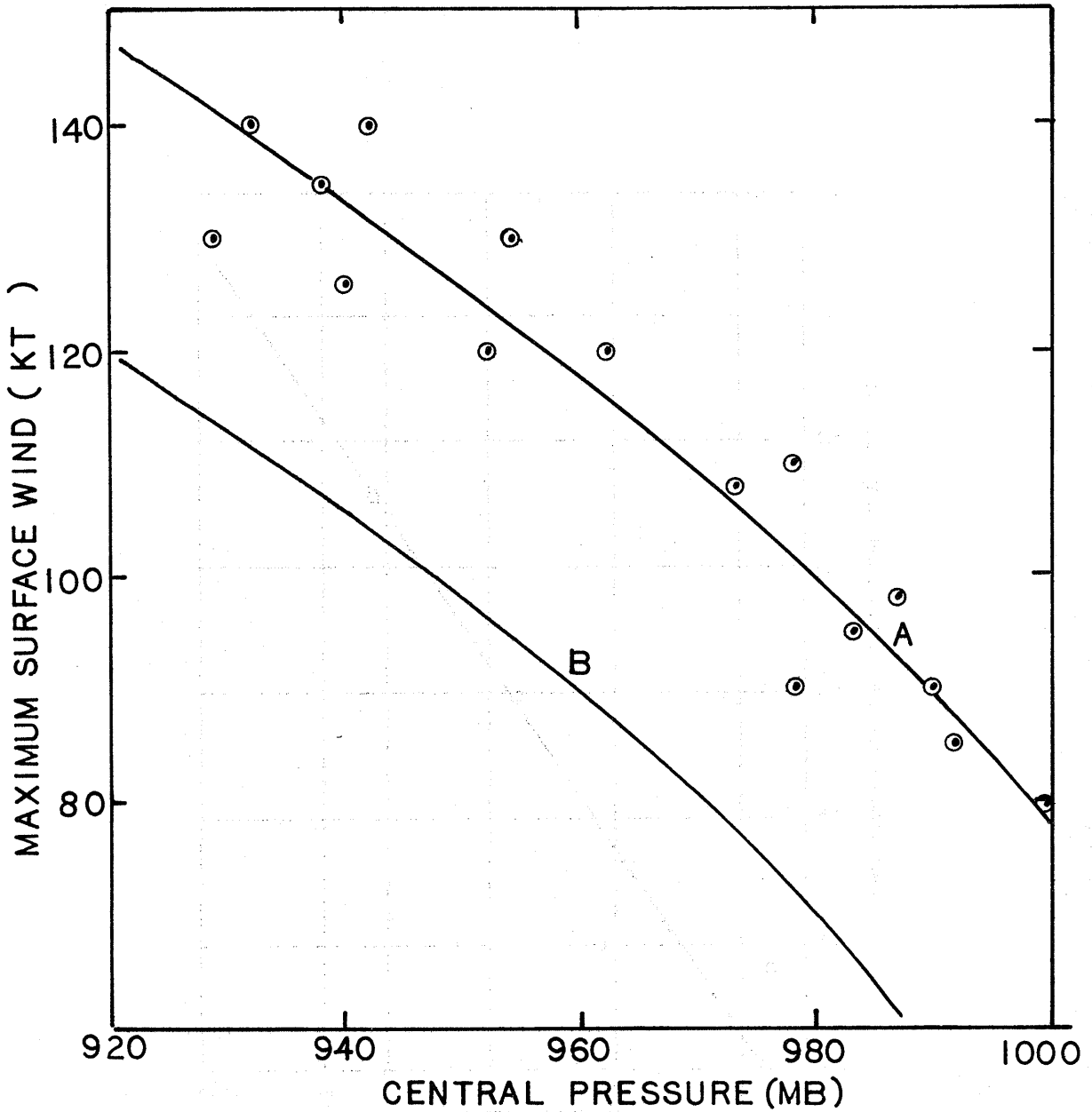
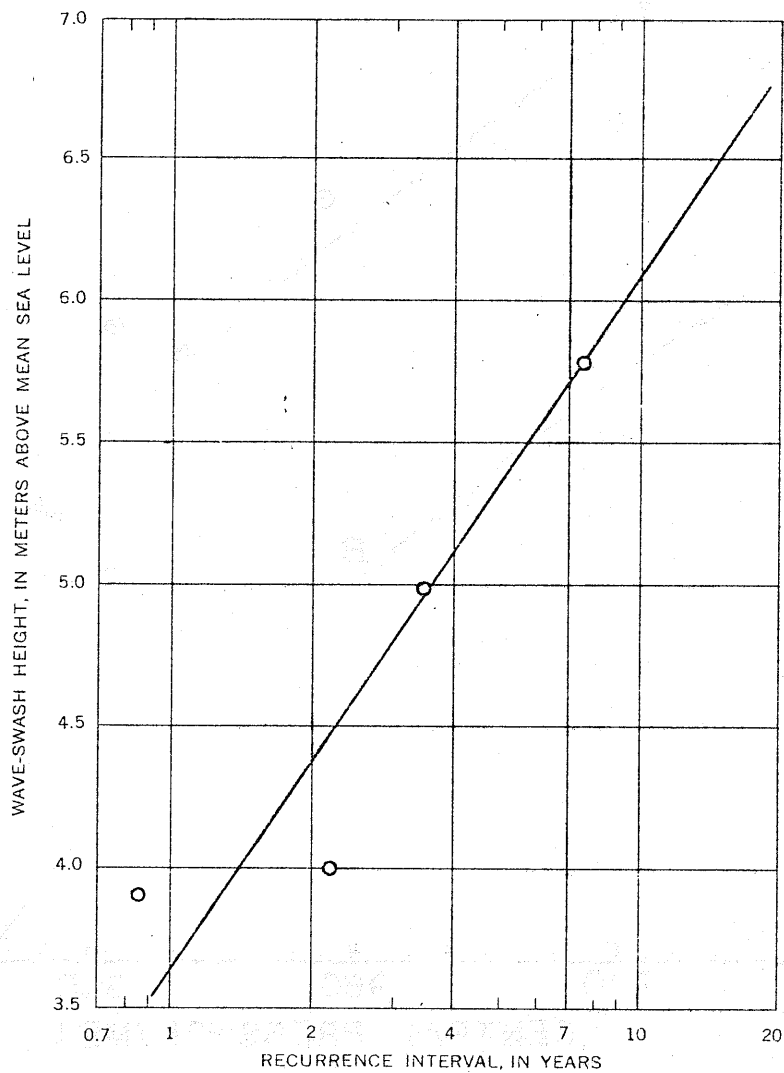
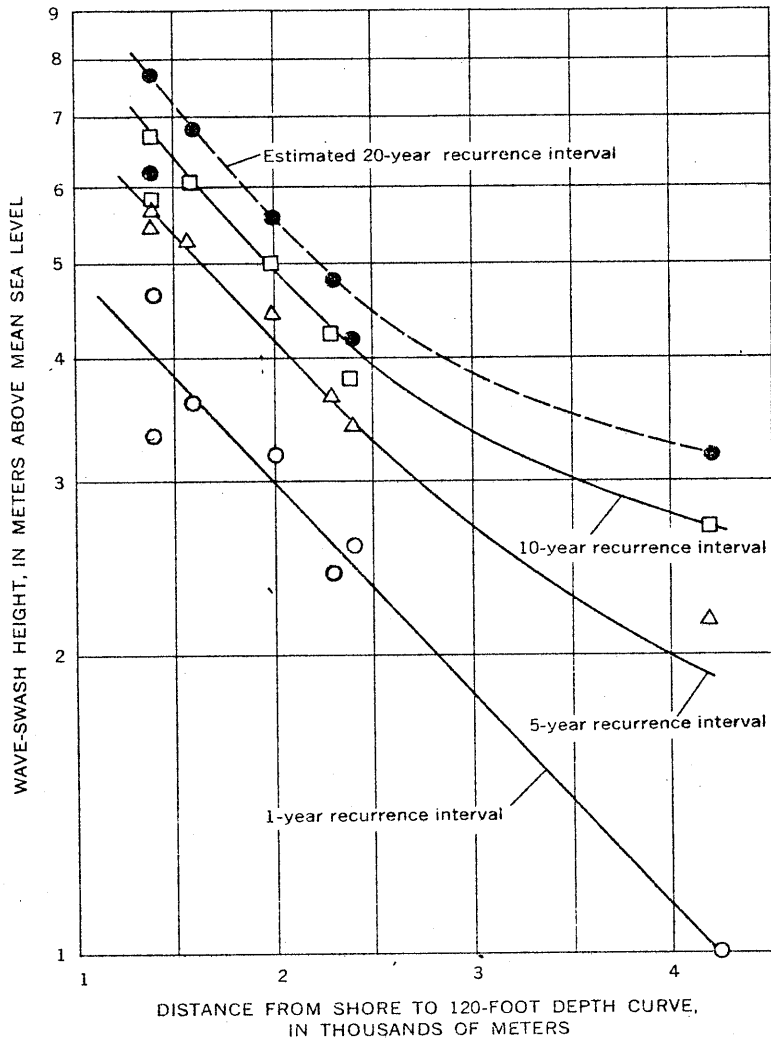


Figure 5-4. Maximum hurricane surface wind vs. central pressure for storms in Table 3-1. Plotted points: maximum wind reported by aircraft. Curve A: eye-fit to these points. Curve B: Maximum wind vs. central pressure relationship from SPLASH model [8] for $R = 15$ n. mi. and forward speed of 14 kt.



Stage-frequency relation of wave swash at Arcibo, longitude 66°43'.

Figure 6-1.---Stage-frequency relationship for wave swash at Arcibo. From [12].



Relation of stage and frequency of wave swash to distance between shoreline and the 120-foot depth curve.

Figure 6-2.---Generalized stage frequencies for wave swash, north coast of Puerto Rico. From [12].